Molecular Therapy
Nucleic Acids
Original Article

Evaluation of *MYBPC3 trans*-Splicing and Gene Replacement as Therapeutic Options in Human iPSC-Derived Cardiomyocytes

Maksymilian Prondzynski,[1,2] Elisabeth Krämer,[1,2] Sandra D. Laufer,[2,3] Aya Shibamiya,[2,3] Ole Pless,[4] Frederik Flenner,[1,2] Oliver J. Müller,[5,6] Julia Münch,[2,7] Charles Redwood,[8] Arne Hansen,[1,2] Monica Patten,[2,7] Thomas Eschenhagen,[1,2] Giulia Mearini,[1,2] and Lucie Carrier[1,2]

[1]Department of Experimental Pharmacology and Toxicology, Cardiovascular Research Center, University Medical Center Hamburg-Eppendorf, 20246 Hamburg, Germany; [2]DZHK (German Centre for Cardiovascular Research), partner site Hamburg/Kiel/Lübeck, 20246 Hamburg, Germany; [3]Hamburg Zentrum für Experimentelle Therapieforschung (HEXT) Stem Cell Facility, University Medical Center Hamburg-Eppendorf, 20246 Hamburg, Germany; [4]Fraunhofer IME Screening-Port, 22525 Hamburg, Germany; [5]Department of Cardiology, Internal Medicine III, University Hospital Heidelberg, 69120 Heidelberg, Germany; [6]DZHK (German Centre for Cardiovascular Research), partner site Heidelberg/Mannheim, 69120 Heidelberg, Germany; [7]University Heart Center Hamburg, 20246 Hamburg, Germany; [8]Radcliffe Department of Medicine, University of Oxford, Oxford OX1 3PA, UK

Gene therapy is a promising option for severe forms of genetic diseases. We previously provided evidence for the feasibility of *trans*-splicing, exon skipping, and gene replacement in a mouse model of hypertrophic cardiomyopathy (HCM) carrying a mutation in *MYBPC3*, encoding cardiac myosin-binding protein C (cMyBP-C). Here we used human induced pluripotent stem cell-derived cardiomyocytes (hiPSC-CMs) from an HCM patient carrying a heterozygous c.1358-1359insC *MYBPC3* mutation and from a healthy donor. HCM hiPSC-CMs exhibited ~50% lower *MYBPC3* mRNA and cMyBP-C protein levels than control, no truncated cMyBP-C, larger cell size, and altered gene expression, thus reproducing human HCM features. We evaluated RNA *trans*-splicing and gene replacement after transducing hiPSC-CMs with adeno-associated virus. *trans*-splicing with 5′ or 3′ pre-*trans*-splicing molecules represented ~1% of total *MYBPC3* transcripts in healthy hiPSC-CMs. In contrast, gene replacement with the full-length *MYBPC3* cDNA resulted in ~2.5-fold higher *MYBPC3* mRNA levels in HCM and control hiPSC-CMs. This restored the cMyBP-C level to 81% of the control level, suppressed hypertrophy, and partially restored gene expression to control level in HCM cells. This study provides evidence for (1) the feasibility of *trans*-splicing, although with low efficiency, and (2) efficient gene replacement in hiPSC-CMs with a *MYBPC3* mutation.

INTRODUCTION

In the last decade, several strategies have been developed to correct or remove gene mutations at the DNA or RNA level, including gene replacement by cDNA overexpression, CRISPR/Cas9 gene editing, exon skipping, spliceosome-mediated RNA *trans*-splicing (*trans*-splicing), and RNAi (as reviewed elsewhere[1–3]). Hypertrophic cardiomyopathy (HCM) is a myocardial disease with a revised estimated prevalence of 1:200 in the general population.[4] It is mainly characterized by hypertrophy of the left ventricle, increased interstitial fibrosis, and diastolic dysfunction.[5] Current therapies, including β-blockers and Ca^{2+}-channel blockers, aim at the relief of symptoms, but they are not curative.[6] HCM is caused by mutations in genes encoding sarcomeric proteins. Among them, *MYBPC3*, encoding cardiac myosin-binding protein C (cMyBP-C), is the most frequently mutated gene.[5,7] To date more than 350 HCM-causing *MYBPC3* mutations have been reported in the literature.[7] The majority of *MYBPC3* mutations are truncating, leading to C-terminal-truncated cMyBP-C proteins, which were never detected in the myocardial tissue of HCM patients.[8]

cMyBP-C is a multidomain protein that plays a role in the regulation of cardiac function and in sarcomeric organization.[9–11] A growing body of evidence indicates that double heterozygous, compound heterozygous, and homozygous mutations in sarcomeric genes are associated with severe forms of cardiomyopathies.[12–14] Specifically, individuals carrying bi-allelic truncating *MYBPC3* mutations presented already at birth with various forms of cardiomyopathies (hypertrophic, dilated, and/or left ventricular non-compaction), which quickly developed into systolic heart failure and death within the first year.[15–17] For these infants, there is no curative therapy other than heart transplant. Recently, proof-of-concept studies reported the feasibility of exon skipping, *trans*-splicing, RNAi, or gene replacement

Received 22 November 2016; accepted 11 May 2017;
http://dx.doi.org/10.1016/j.omtn.2017.05.008.

Correspondence: Lucie Carrier, Department of Experimental Pharmacology and Toxicology, University Medical Center Hamburg-Eppendorf, Martinistraße 52, 20246 Hamburg, Germany.
E-mail: l.carrier@uke.de
Correspondence: Giulia Mearini, Department of Experimental Pharmacology and Toxicology, University Medical Center Hamburg-Eppendorf, Martinistraße 52, 20246 Hamburg, Germany.
E-mail: g.mearini@uke.de

as gene therapy options in HCM mouse models.[18–21] To move this concept toward clinical application, advantage could be taken from the use of human induced pluripotent stem cell-derived cardiomyocytes (hiPSC-CMs). These cells have already been used for disease modeling of long-QT syndrome,[22,23] dilated cardiomyopathy,[24–26] and HCM,[27–29] and they could be used as a platform for testing different gene therapy options. In the present study, we evaluated the feasibility and efficiency of *MYBPC3* *trans*-splicing and gene replacement strategies in hiPSC-CMs obtained from a healthy donor and an HCM patient harboring a heterozygous truncating mutation in the *MYBPC3* gene.

trans-splicing involves two separate mRNAs, the target endogenous mutant pre-mRNA and an exogenous wild-type (WT) pre-*trans*-splicing molecule (PTM; as reviewed elsewhere[30,31]). After gene transfer of the PTMs, a splice event in *trans* can occur between the two molecules, resulting in a chimeric repaired mRNA, which is then translated into a corrected protein (Figure S1A). Beside the WT coding sequence, PTMs carry strong splice sequences and a binding domain for specific recognition of the target. Depending on the position of the mutation in the pre-mRNA, *trans*-splicing can occur in 5′ or 3′ mode, and PTMs will contain a splice donor or acceptor site, respectively. In the gene replacement approach, a correct copy of the defective gene, i.e., full-length WT cDNA, is provided to the cell in order to replace the non-functional and/or missing protein (Figure S1B; as reviewed elsewhere[32,33]). In the present work, PTMs carrying each half of the *MYBPC3* coding sequence and full-length WT *MYBPC3* cDNA were packaged into the adenovirus-associated virus serotype 9-SRLSPPS (hereafter AAV),[34] and analyses were done 7 days after AAV transduction.

RESULTS

HCM hiPSC-CMs Show Hypertrophy and cMyBP-C Haploinsufficiency

At the time of septal myectomy, the patient had an interventricular septal thickness of 26 mm, ejection fraction of >60%, and a left ventricular outflow gradient of 85 mmHg. Genetic testing of genomic DNA with a panel of 19 HCM genes revealed an insertion of a C in exon 16 of the *MYBPC3* gene (c.1358_1359insC; Figure S2) on one allele of the HCM patient. This variant was not found in the Exome Association Consortium (ExAC) Browser, which harmonized sequencing data from more than 60,000 unrelated individuals (http://exac.broadinstitute.org/), supporting its causal effect. The mutation induced a frameshift and a premature termination codon (PTC) in exon 16. At the protein level, an amino acid substitution at position 454 was followed by 21 new amino acids (p.Val454CysfsX21) and truncation in the C3 domain of cMyBP-C.

Dermal fibroblasts from the HCM patient and from a healthy donor (control) were reprogrammed into hiPSCs, followed by differentiation into CMs (see the Materials and Methods). Both HCM and control hiPSC-CMs were seeded in a confluent monolayer and cultured for 7 days. hiPSC-CMs of both cell lines exhibited spontaneous beating (data not shown). After fixation, immunofluorescence analysis with antibodies directed against cMyBP-C and α-actinin showed a cross-striated pattern, indicating proper formation of sarcomeres (Figure 1A). Cell size, as determined by automated analysis of large numbers of cells (see the legend of Figure 1B), was significantly higher in HCM than in control hiPSC-CMs (3,656 ± 201 μm^2 versus 2,213 ± 145 μm^2; Figure 1B). Total *MYBPC3* mRNA level was 50% lower in HCM than in control cells (Figure 1C). Mutant *MYBPC3* mRNA was not detected by Sanger sequencing or with a specific Taqman probe (data not shown). The amount of cMyBP-C protein normalized to α-actinin tended to be lower ($p = 0.064$) in HCM than in control hiPSC-CMs (Figures 1D and 1E). No truncated protein (~52 kDa) was detected in HCM cells (data not shown). The disease phenotype of HCM hiPSC-CMs was further evaluated by gene expression profile of 49 proteins involved in the regulation of cardiac hypertrophy and contraction with the nanoString nCounter Elements technology (Figure S3; Table S1). Most of the proteins associated with hypertrophy, cardiomyopathy, and/or PI3K-Akt signaling exhibited higher mRNA levels in HCM than in control CMs (green bars), whereas many proteins involved in excitation-contraction coupling or adrenergic signaling had lower mRNA levels in HCM than in control CMs (red bars).

5′ *trans*-Splicing Is Feasible in hiPSC-CMs

We designed a 5′ PTM that would be able, in principle, to repair all *MYBPC3* mutations contained in the first half of the gene. It carried the WT *MYBPC3* cDNA sequence from exon 1 to exon 21 under the control of a CM-specific promoter (*TNNT2*, human cardiac troponin T; Figure 2A). The 5′ PTM included a binding domain for base pairing with a complementary sequence (120 nt) in intron 21 of the *MYBPC3* gene, a canonical 5′ splice site sequence followed by a downstream intronic sequence enhancer element, which has been shown to markedly increase *trans*-splicing efficiency (Figure S4A).[35] To allow specific detection of *MYBPC3* *trans*-spliced mRNA and cMyBP-C protein, we included a FLAG-tag sequence at the N terminus of the coding sequence (Figure 2A). To prevent translation of the PTM, we removed the polyA signal as described previously.[19] For gene transfer in hiPSC-CMs, 5′ PTMs were packaged into AAV. Beforehand, we tested the transduction efficiency of different MOIs of AAV-*TNNT2*-GFP in control hiPSC-CMs. The MOI of 10,000 proved to transduce >80% of hiPSC-CMs after 7 days of transduction (Figure S5).

Control hiPSC-CMs were then transduced with AAV-5′ PTM or AAV-Mock (empty virus; both at an MOI of 10,000) and cultured for 7 days in 2D. Using PCR primers that amplify only *trans*-spliced *MYBPC3* transcript (Figure 2B), we obtained a specific fragment only in AAV-5′ PTM-transduced hiPSC-CMs, but not in non-transduced or mock-transduced hiPSC-CMs (Figure 2C). After agarose gel extraction, sequencing of the 2,180-bp *trans*-spliced *MYBPC3* fragment validated the presence of the FLAG-tag (Figure S6A). To evaluate the effect of *trans*-splicing on *cis*-splicing, total *MYBPC3* mRNA (= *trans*-spliced + endogenous) was amplified with primers in exon 1 and exon 23 (Figure 2B). A specific amplicon was obtained in all samples without a major intensity difference among them (Figure 2C). To estimate the efficiency of 5′ *trans*-splicing, cDNA from AAV-5′

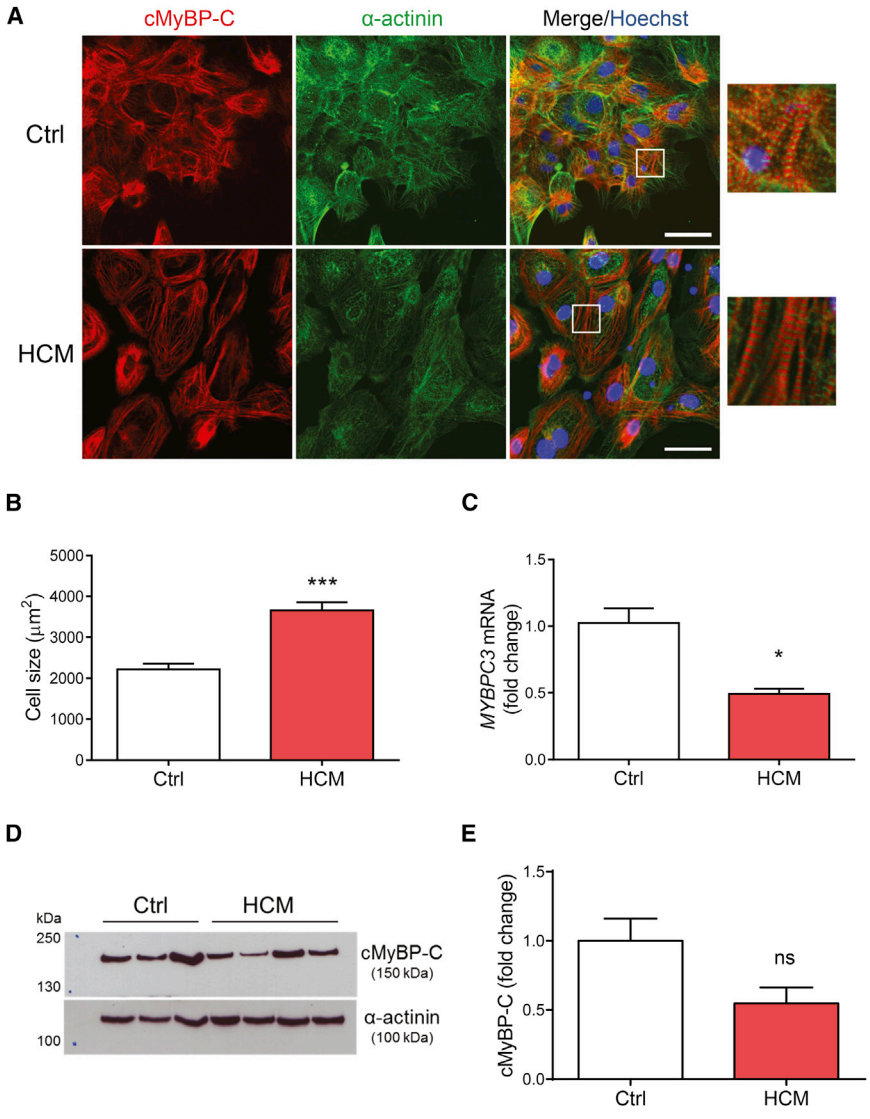

Figure 1. Phenotypic Characterization of HCM hiPSC-Derived Cardiomyocytes

Patient-specific (HCM) and control (Ctrl) hiPSC-derived cardiomyocytes (hiPSC-CMs) were seeded in a confluent monolayer, cultured for 7 days, and prepared for subsequent analysis. (A) Representative immunofluorescence images of HCM and control hiPSC-CMs. Both cell lines were stained with antibodies directed against cMyBP-C (red), α-actinin (green), and with Hoechst33342 for nuclear staining (blue; scale bars, 50 μm). Higher magnification images of a few sarcomeres are shown on the right panels. (B) Quantification of CM cell size. Control and HCM hiPSC-CMs were seeded in 96-well plates at a density of 10,000 cells/well, cultured for 7 days, and stained with an antibody against α-actinin. Cell size was measured in 27–51 fields/well in both groups. Control hiPSC-CMs were evaluated from 33 wells of three independent experiments and HCM hiPSC-CMs from 21 wells of two independent experiments, for a total of 28,336 and 12,874 CMs, respectively. Images were taken with the Opera High-Content Screening System (PerkinElmer), and the analyses were performed with the Columbus Image Data Management and Analysis System. (C) Evaluation of *MYBPC3* mRNA levels determined by qRT-PCR with SYBR Green in control and HCM hiPSC-derived CMs (n = 3–5, with n = number of wells from one transduction experiment). (D) Western blot of control and HCM hiPSC-CMs stained with antibodies directed against cMyBP-C. α-actinin was used as the loading control. (E) Quantification of cMyBP-C protein levels in control and HCM hiPSC-CMs normalized to α-actinin and related to control (n = 3–4, with n = number of wells from two independent transduction experiments). Values are expressed as mean ± SEM (*$p < 0.05$ and ***$p < 0.001$, unpaired Student's t test). cMyBP-C, cardiac myosin-binding protein C; CMs, cardiomyocytes; Ctrl, control.

PTM-transduced hiPSC-CMs was used to amplify either *trans*-spliced or total *MYBPC3* mRNA by PCR (25 cycles). PCR fragments were column-purified and further analyzed by qPCR using a common primer pair for amplification of the same fragment in all *MYBPC3* transcripts. The percentage of *trans*-spliced *MYBPC3* mRNA was calculated using a standard dilution ($2 \times 10^9 - 2 \times 10^1$ copy number) of a plasmid encoding the full-length WT *MYBPC3* cDNA. Samples and standards were amplified with the same primer pair, enabling us to specifically calculate a 5′ *trans*-splicing efficiency of 0.96% (Figure 2D). FLAG immunoprecipitation experiments to detect *trans*-spliced cMyBP-C protein were not successful (data not shown), probably due to low *trans*-splicing efficiency.

3′ *trans*-Splicing Is Feasible in hiPSC-CMs

We designed a 3′ PTM, that would principally be able to repair all *MYBPC3* mutations contained in the second half of the gene. It carried the WT *MYBPC3* cDNA sequence from exon 22 to exon 34 under the control of the *TNNT2* promoter (Figure 3A). The *MYBPC3* cDNA sequence was FLAG-tagged at the C terminus to discriminate the *trans*-spliced *MYBPC3* mRNA and cMyBP-C protein from endogenous ones. To prevent any translation of the 3′ PTM, no ATG sequence was introduced. To allow 3′ *trans*-splicing, we also inserted in the 3′ PTM a binding domain (same sequence as in 5′ PTM) targeting intron 21 followed by a linker sequence, a branch point, a polypyrimidine tract, and a 3′ splice site (Figure S4B). After packaging in AAV, control hiPSC-CMs were transduced with AAV-3′ PTM or AAV-Mock (MOI 10,000), and they were cultured for 7 days in 2D prior to collection. Primer pairs for detection of *trans*-spliced or total *MYBPC3* mRNA are shown in Figure 4B. A specific 1,874-bp amplicon was obtained in the AAV-3′ PTM-transduced sample with primers designed to recognize *trans*-spliced *MYBPC3* mRNA. Sequencing of this amplicon validated the presence of the FLAG sequence (Figures 3B and 3C; Figure S6B). A fragment of similar size was detected in the non-transduced sample, but sequencing did not reveal the FLAG sequence (data not shown).

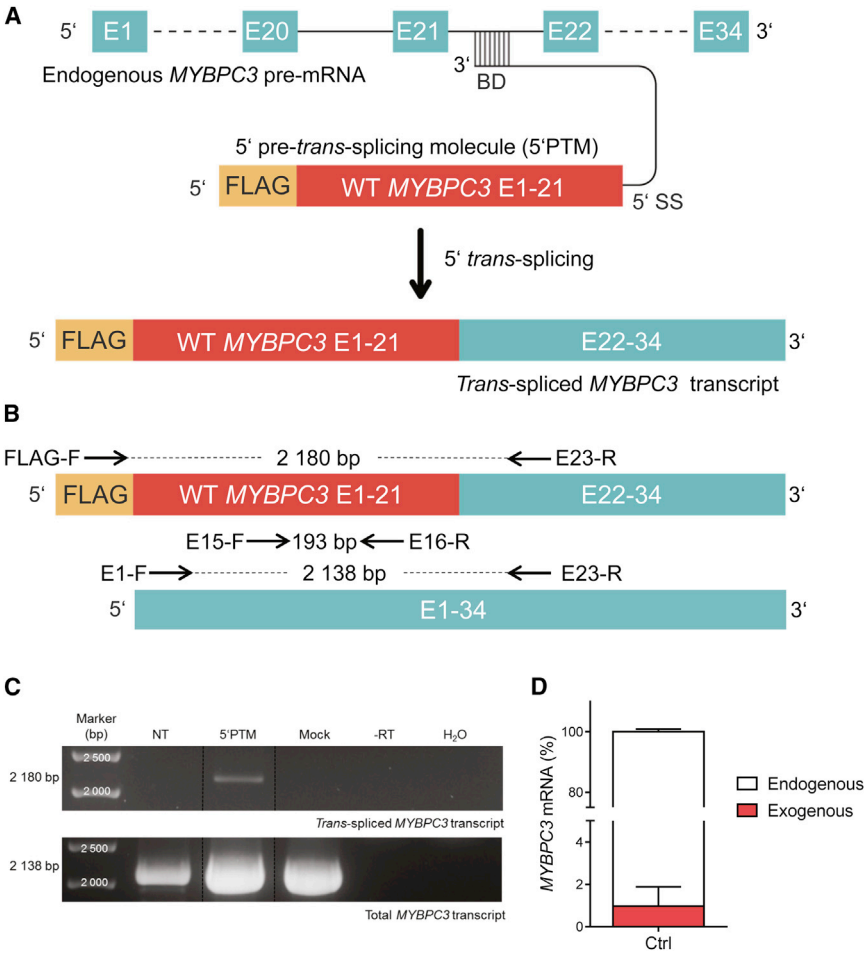

Figure 2. 5′ *trans*-Splicing in Control hiPSC-Derived Cardiomyocytes

(A) Schematic representation of 5′ *trans*-splicing. 5′ pre-*trans*-splicing molecules (5′ PTMs) carry a 5′ FLAG-tagged wild-type (WT) *MYBPC3* cDNA sequence from exon 1 to exon 21, conserved 5′ splice donor site (5′SS) sequences, and a binding domain (BD) targeting intron 21. Upon successful binding of 5′ PTM to the endogenous *MYBPC3* pre-mRNA, 5′ *trans*-splicing can occur and results in a *trans*-spliced *MYBPC3* mRNA. (B) Schematic illustration of primer pairs used to amplify either only *trans*-spliced or *trans*-spliced and/or endogenous (total) *MYBPC3* mRNAs. The primer pair FLAG-F/E23-R was used to generate a 2,180-bp fragment corresponding to the *trans*-spliced *MYBPC3* mRNA. *trans*-spliced and/or endogenous *MYBPC3* mRNA was amplified either using the primer pair E1-F/E23-R (2,138-bp fragment) or the primer pair E15-F/E16-R (193-bp fragment). (C) hiPSC-derived cardiomyocytes (hiPSC-CMs) were transduced with AAV-5′ PTM or AAV-Mock (*TNNT2* promoter without insert) at an MOI of 10,000 and cultured in 2D for 7 days prior to harvesting. Representative agarose gel of RT-PCR, using specific primer pairs for *trans*-spliced and total *MYBPC3* mRNA, is shown (n = 5, from three independent transductions). (D) Determination of the percentage of *trans*-spliced *MYBPC3* mRNA by qRT-PCR. In a first round of PCR, either *trans*-spliced (FLAG-F/E23-R primers) or total (E1-F/E23-R primers) *MYBPC3* mRNAs were amplified from cDNA of AAV-5′ PTM-transduced hiPSC-CMs. PCR fragments were column-purified and used in qPCR, together with a standard dilution of a plasmid encoding full-length wild-type *MYBPC3* cDNA, using a common primer pair (E15-F/E16-R primers). Data are expressed as mean ± SEM with n = 3 (three wells of one transduction experiment). AAV, adeno-associated virus; bp, base pair; CMs, cardiomyocytes; E, exon; F, forward; hiPSC, human induced pluripotent stem cell; NT, non-transduced; MOI, multiplicity of infection; R, reverse; RT, reverse transcriptase; WT, wild-type.

Similarly, PCR fragments also appeared in the AAV-3′ PTM-transduced but without reverse transcriptase sample, indicating nonspecific binding of the primers to the endogenous mRNA. RT-PCR with a primer pair that amplified total *MYBPC3* mRNA showed a signal of similar intensity in non-transduced and in AAV-transduced samples (Figure 3C). As was done for 5′ *trans*-splicing, the efficiency of 3′ *trans*-splicing was determined by qRT-PCR with a standard dilution ($2 \times 10^9 - 2 \times 10^1$ copy number) of the same plasmid carrying the full-length WT *MYBPC3* cDNA. The concentration of *trans*-spliced *MYBPC3* mRNA reached 1% of the total (Figure 3D). Similar to 5′ *trans*-splicing, the *trans*-spliced cMyBP-C protein was not detected after FLAG immunoprecipitation (data not shown).

Gene Replacement in HCM hiPSC-CMs Partially Corrects cMyBP-C Haploinsufficiency and Reduces Cell Hypertrophy

To evaluate a gene replacement therapy option, the FLAG-tagged WT *MYBPC3* cDNA under the control of the *TNNT2* promoter was packaged in AAV (AAV-FLAG-*MYBPC3*). After transduction (MOI 10,000) of control and HCM hiPSC-CMs, cells were cultured for 7 days in 2D prior to harvesting. RT-PCR with specific primers for exogenous *MYBPC3* transcript revealed a specific fragment in both control and HCM transduced hiPSC-CMs (Figures 4A and 4B). A signal of lower intensity was also obtained in AAV-transduced samples, which were not retrotranscribed, corresponding to the transgene. The transcription of the entire FLAG-*MYBPC3* cDNA sequence was also validated (data not shown). Total *MYBPC3* transcript was amplified using a common primer pair in all samples, transduced or not (Figures 4A and 4B). To quantify the overall level of *MYBPC3* mRNA after transduction, a qRT-PCR was performed with a primer pair recognizing both exogenous and endogenous *MYBPC3* mRNA transcripts (Figures 4A and 4C). About 2.5-fold overexpression of *MYBPC3* was obtained in both control and HCM transduced hiPSC-CMs over the non-transduced cells (Figure 4C). To evaluate the efficiency of gene replacement, RT-PCR with specific primers to amplify either exogenous or total *MYBPC3* transcripts was performed in control and HCM transduced samples. PCR fragments were column-purified and used further for qPCR with a common primer pair, together with a standard dilution curve of a plasmid carrying

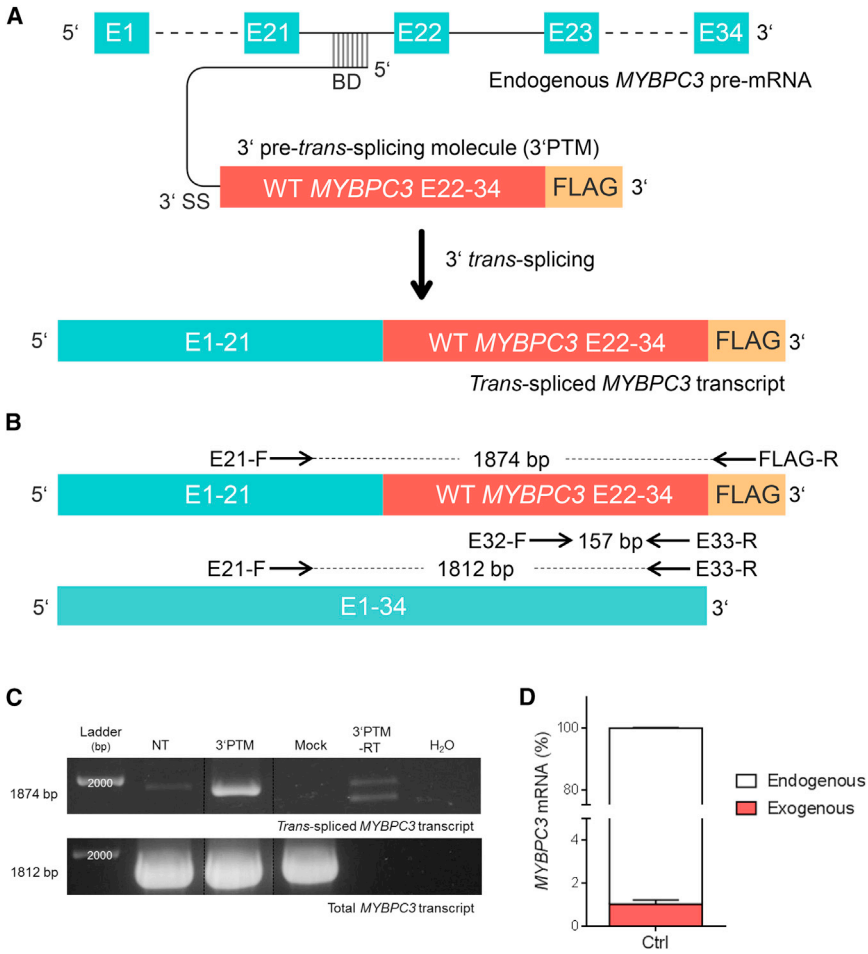

Figure 3. 3′ *trans*-Splicing in Control hiPSC-Derived Cardiomyocytes

(A) Schematic illustration of 3′ *trans*-splicing. 3′ pre-*trans*-splicing molecules (3′ PTMs) contain a BD complementary to *MYBPC3* intron 21, conserved 3′ splice donor site sequences (3′SS), and a 3′-FLAG-tagged wild-type (WT) *MYBPC3* cDNA sequence from exon 22 to exon 34. Upon successful binding of the 3′ PTM to the endogenous *MYBPC3* pre-mRNA, 3′ *trans*-splicing can occur and results in *trans*-spliced *MYBPC3* mRNA. (B) Schematic representation of primer pairs used to amplify either only *trans*-spliced *MYBPC3* mRNA or *trans*-spliced and/or endogenous (total) *MYBPC3* mRNA. The primer pair E21-F/FLAG-R amplifies a 1,874-bp fragment specific of *trans*-spliced *MYBPC3* mRNA. The primer pairs E21-F/E33-R and E33-F/E33-R amplify in both *trans*-spliced and endogenous *MYBPC3* mRNA a 1,812-bp and a 157-bp fragment, respectively. (C) Control hiPSC-CMs were transduced with AAV-3′ PTM or AAV-Mock (MOI 10,000) for 1 week prior to harvesting. Representative agarose gel of RT-PCR, using specific primer pairs for *trans*-spliced and total *MYBPC3* mRNA, is shown (n = 9 from four independent transductions). (D) Determination of the percentage of *trans*-spliced *MYBPC3* mRNA by qRT-PCR was performed as described in Figure 2D, with the common primer pair E33-F/E33-R. Data are expressed as mean ± SEM with n = 5 (five wells of one transduction experiment). bp, base pair; CMs, cardiomyocytes; E, exon; F, forward; hiPSC, human induced pluripotent stem cell; NT, non-transduced; MOI, multiplicity of infection; R, reverse; RT, reverse transcriptase; WT, wild-type.

the full-length wild-type *MYBPC3* cDNA sequence ($2 \times 10^9 - 2 \times 10^1$ copy number). In control and HCM hiPSC-CMs, exogenous *MYBPC3* transcript level reached 70% and 57% of total, respectively (Figure 4D). The level of cMyBP-C protein was determined by western blot analysis in protein samples, normalized to α-actinin content and related to non-transduced control hiPSC-CM sample (Figures 4E and 4F). The total cMyBP-C protein level did not differ between transduced and non-transduced control hiPSC-CMs. In contrast, cMyBP-C protein level was 2.5-fold higher ($p < 0.05$, Student's t test) in transduced than in non-transduced HCM hiPSC-CMs, reaching 81% of the cMyBP-C level of the non-transduced control sample (Figures 4E and 4F).

Sarcomere organization after transduction of control and HCM hiPSC-CMs with AAV-FLAG-*MYBPC3* was evaluated by immunofluorescence analysis with anti-FLAG and anti-α-actinin antibodies. FLAG-cMyBP-C protein was properly organized in doublets at the A-band of the sarcomere, well alternating with α-actinin located at the Z-disk (Figure 5A). Finally, we evaluated the impact of *MYBPC3* gene transfer on cell size. Cell size was significantly higher in non-transduced HCM than in control hIPSC-CMs (Figure 5B). *MYBPC3* gene transfer did not affect cell size in control hiPSC-CMs (2,715 ± 168 μm^2 versus 2,665 ± 120 μm^2 in non-transduced control). In contrast, cell size was significantly lower in *MYBPC3*-transduced than in non-transduced HCM hiPSC-CMs (3,205 ± 139 μm^2 versus 4,409 ± 217 μm^2), and it did not differ from non-transduced control hiPSC-CMs (Figure 5B). *MYBPC3* gene replacement lowered mRNA levels of several proteins involved in cardiomyopathy and PI3K-Akt signaling, and it increased mRNA levels of calcium-handling proteins in HCM hiPSC-CMs (Figure 6).

DISCUSSION

In this study, we report the principal feasibility of two gene therapy options for HCM in hiPSC-CMs from a healthy donor and an HCM patient carrying a *MYBPC3* truncating mutation. While our data suggest that *trans*-splicing efficiency is too low to be a therapeutic option to treat severe forms of HCM, the *MYBPC3* gene replacement strategy looks promising, particularly for its ability to circumvent haploinsufficiency of cMyBP-C (restoration of a correct amount of protein) and to reduce CM hypertrophy. Numerous studies have used hiPSC-CMs as a tool for disease modeling of different cardiac diseases, including HCM with *MYBPC3* mutations.[22–29,36–39]

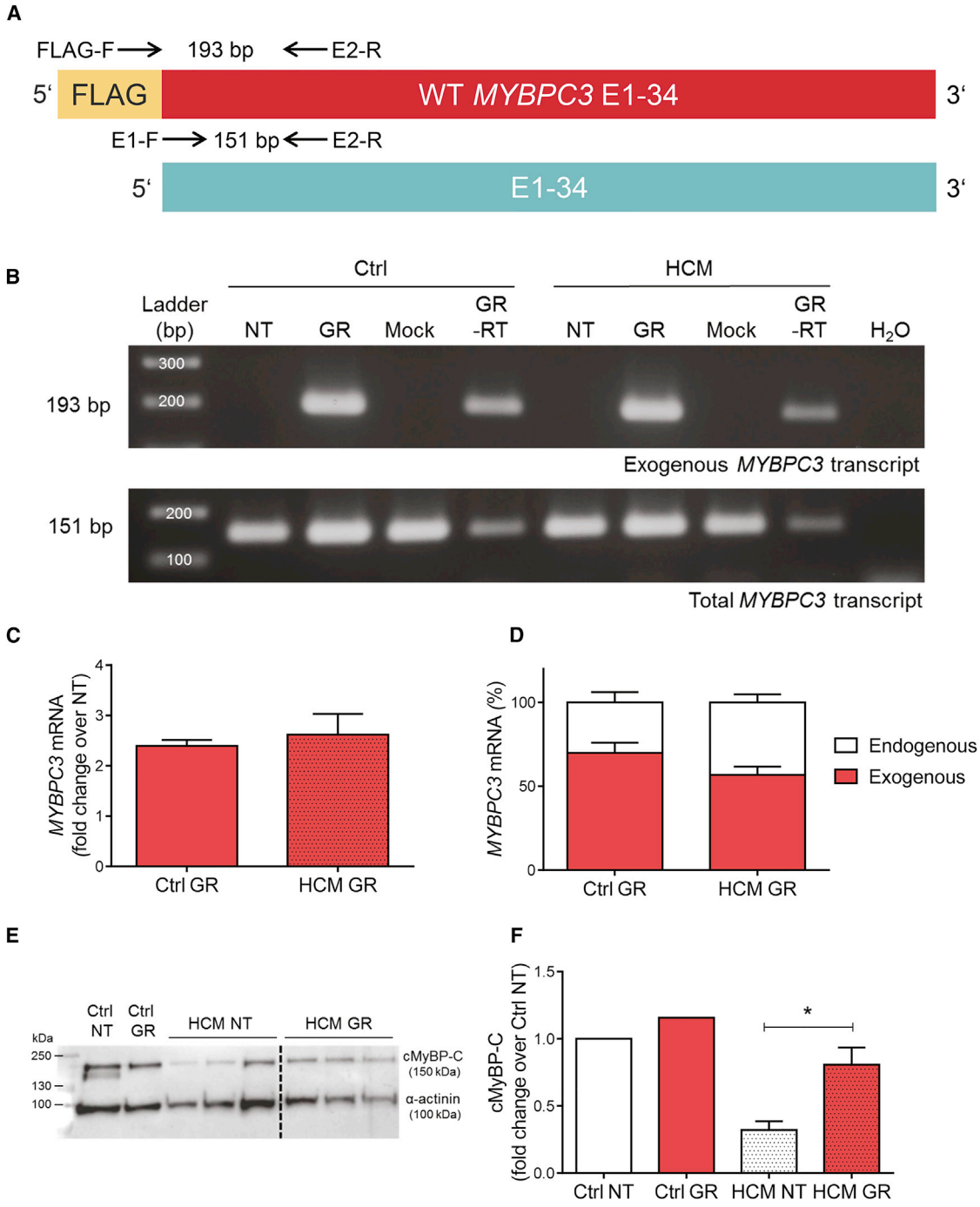

Figure 4. Proof-of-Concept of *MYBPC3* Gene Replacement in Human iPSC-Derived Cardiomyocytes

(A) Schematic illustration of full-length wild-type (WT) exogenous and total *MYBPC3* cDNA/mRNA sequence (exons 1–34). Location of primer pairs and size of amplicons are shown. The primer pair FLAG-F/E2-R amplifies exclusively the exogenous *MYBPC3* sequence (amplicon size: 193 bp). The primer pair E1-F/E2-R is suitable for amplification of both exogenous and endogenous (total) *MYBPC3* sequence (amplicon size: 151 bp). (B) Control and HCM hiPSC-CMs were transduced with AAV-FLAG-*MYBPC3* (GR) or AAV-Mock (Mock) at an MOI of 10,000 and cultured in 2D for 7 days before harvesting. Representative RT-PCR using primers shown in (A) for specific amplification is shown (n = 3, one well each from three independent transductions). (C) Evaluation of *MYBPC3* transcript levels in GR-transduced control and HCM hiPSC-CMs by qRT-PCR with a common primer pair (n = 3–5, with n = number of wells of one transduction experiment). (D) Determination of the percentage of exogenous *MYBPC3* mRNA by qRT-PCR. In a first round of RT-PCR, either exogenous (FLAG-F/E2-R primers) or total (E1-F/E2-R primers) *MYBPC3* transcripts were amplified in control and HCM GR samples. After column purification of PCR fragments, a qPCR with a common primer pair (E1-F/E2-R) was performed together with a standard dilution of a plasmid encoding full-length

(legend continued on next page)

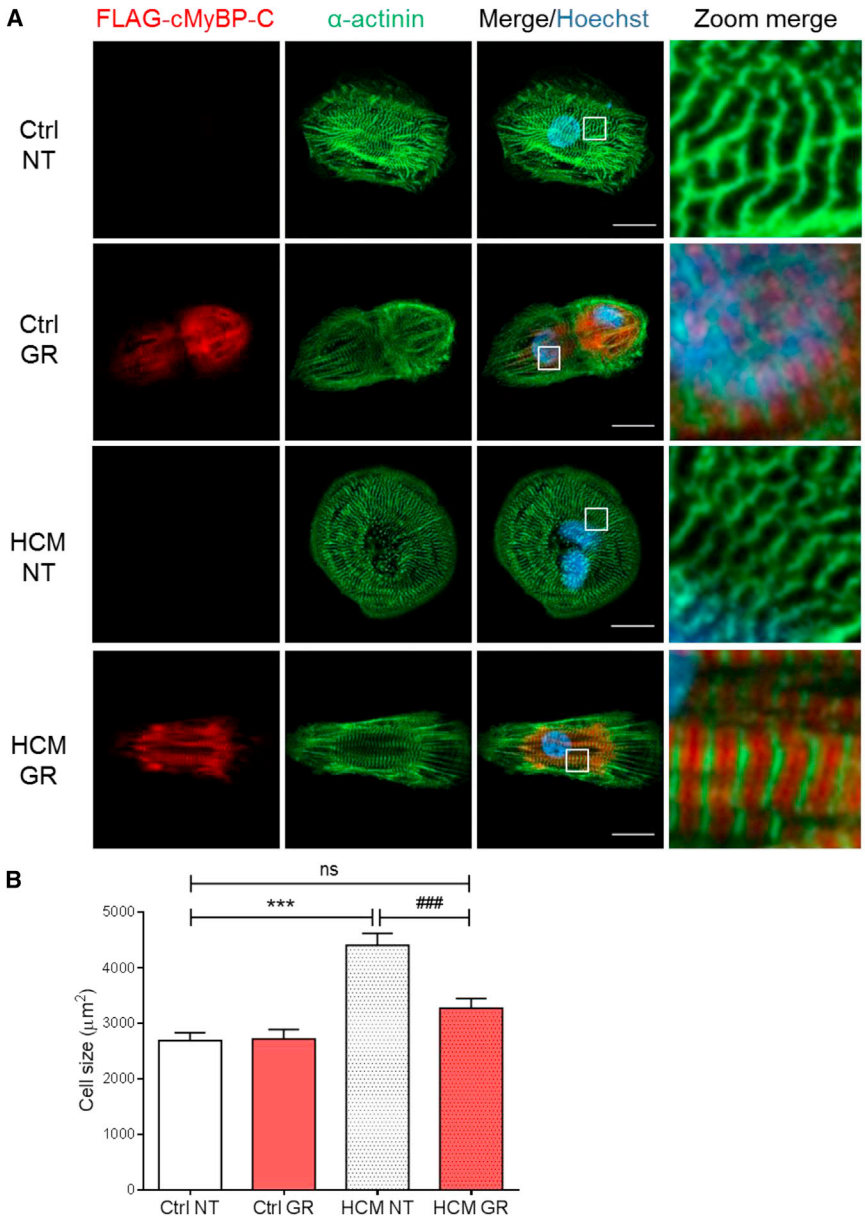

Figure 5. Phenotypic Characterization of Control and HCM hiPSC-Derived Cardiomyocytes after *MYBPC3* Gene Transfer

(A) Representative images of non-transduced (NT) and transduced (GR) control (Ctrl) and HCM hiPSC-CMs after immunofluorescence staining with anti-FLAG and anti-α-actinin antibodies. Images were taken with a Zeiss LSM 800 microscope (scale bars, 20 μm). Higher magnification images of a few sarcomeres are shown on the right panel. (B) Quantification of CM cell size. NT and GR control and HCM hiPSC-CMs were seeded in 96-well plates at a density of 10,000 cells/well, cultured for 1 week, and stained with antibodies against FLAG-tag and α-actinin. Low-resolution images of >100 cells in each group from six wells of one experiment each (Ctrl NT n = 108; Ctrl GR n = 110; HCM NT n = 114; HCM GR n = 133) were taken with the Zeiss LSM 800 microscope and analyzed with Fiji software (ImageJ). Data are expressed as mean ± SEM (***$p < 0.001$, two-way ANOVA plus Bonferroni post-test; ###$p < 0.001$, unpaired Student's t test).

However, so far only one study used the gene replacement strategy to correct a phospholamban (*PLN*) mutation associated with dilated cardiomyopathy in vitro.[39]

We believe that the truncating p.Val454CysfsX21 *MYBPC3* mutation, described here for the first time, is HCM causing for the following reasons. First, truncating *MYBPC3* mutations were reported to have a >110-fold higher odds ratio to cause HCM.[40] Second, this specific mutation was not found in the population of about 60,000 unrelated individuals of the ExAC Browser (http://exac.broadinstitute.org/). HCM hiPSC-CMs revealed larger cell size, higher mRNA levels of proteins associated with hypertrophy, such as four and a half LIM domains 1 (*FHL1*), S100 calcium-binding protein A4 (*S100A4*), and connective tissue growth factor (*CTGF*), and lower mRNA levels of proteins involved in calcium handling, such as *PLN*, SERCA2A (*ATP2A2*), ryanodine receptor (*RYR2*), and inhibitor 1 (*PPP1R1A*) than control CMs, all hallmarks of HCM. This is in agreement with previous findings using HCM hiPSC-CMs or human embryonic stem cell (hESC) carrying *MYBPC3* mutations.[28,29,37,41] While Dambrot et al.[37] described that the supplementation of serum in culture medium masks the hypertrophic phenotype in 2D culture of hiPSC-CMs, in the present study the enlarged cell size was evident already in the presence of serum, as also reported by Ojala et al.[28]

In addition to hypertrophy, the HCM CMs used in the present work presented another hallmark of the *MYBPC3*-causing HCM, namely haploinsufficiency (for review, see Marston et al.[42]). Indeed, the amounts of *MYBPC3* mRNA and cMyBP-C protein were ~50% of

WT *MYBPC3* cDNA (n = 3, three wells of one transduction experiment). (E) Western blot performed on pooled protein samples (n = 6, from three independent transduction experiments) of non-transduced (NT) or transduced (GR) control and single protein samples (n = 3, three wells of one transduction experiment) of HCM hiPSC-CMs with anti-cMyBP-C and anti-α-actinin antibodies. (F) Quantification of cMyBP-C level normalized to α-actinin and related to control NT pooled sample. Data are expressed as mean ± SEM (*$p < 0.05$, unpaired Student's t test). E, exon; F, forward; NT, non-transduced; MOI, multiplicity of infection; R, reverse; WT, wild-type.

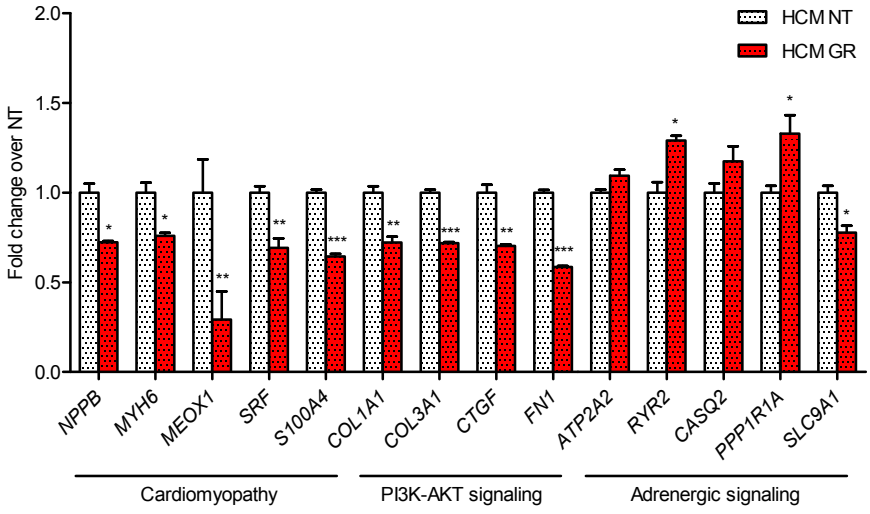

Figure 6. Gene Expression Analysis of HCM hiPSC-Derived Cardiomyocytes in the Absence of or after *MYBPC3* Gene Transfer

The mRNA levels of transduced (GR) and non-transduced (NT) HCM hiPSC-CMs were determined with the nanoString nCounter Elements technology, normalized to housekeeping genes, and related to NT CMs. Data are expressed as mean ± SEM (*$p < 0.05$, **$p < 0.01$, and ***$p < 0.001$, unpaired Student's t test; n = 3, with n = number of wells from one transduction experiment).

the control hiPSC-CMs. Furthermore, the mutant nonsense mRNA was not detected, suggesting that it is degraded by the nonsense-mediated mRNA decay (NMD), as previously shown in *Mybpc3*-targeted knockin HCM mice.[43] The location of the PTC at >50–55 nt upstream of the most 3′ exon-exon junction perfectly matches the NMD rules,[44] therefore supporting its NMD-mediated degradation. The expected 52-kDa truncated cMyBP-C protein was also not detected by western blot, in agreement with previous observations in human myocardial samples with truncating *MYBPC3* mutations.[8,45] Thus, the combination of a unique truncating *MYBPC3* mutation, cMyBP-C haploinsufficiency, and CM hypertrophy makes this hiPSC cell line a good test bed for the application of different treatment options for HCM.

In the last years, mRNA *trans*-splicing has been evaluated both in vitro and in vivo as an alternative option for currently incurable genetic diseases, such as Duchenne muscular dystrophy and spinal muscular atrophy (as reviewed elsewhere[30,31]). In the case of HCM-associated *MYBPC3* mutations, the *trans*-splicing approach was appealing because by generating only two PTMs covering the first and the second half of the *MYBPC3* mRNA, one could principally repair all the mutations and, therefore, treat 40%–60% of all HCM patients.[6,7] In addition, and in contrast to exon skipping mediated by antisense oligonucleotides (AONs), *trans*-splicing is expected to result in a repaired full-length and functional cMyBP-C protein. Furthermore, FDA or EMA authorization for marketing of two PTMs as new medicinal products would be easier and quicker than for several AONs.

In the present study, we showed the feasibility of both 5′ and 3′ *trans*-splicing in control hiPSC-CMs. However, we did not test these approaches in HCM hiPSC-CMs, since the efficiency of the process was low and we were unable to detect repaired cMyBP-C protein. This supports our previous data obtained in vivo in *Mybpc3*-targeted knockin mice, in which the low amount of repaired cMyBP-C protein produced by 5′ *trans*-splicing was not sufficient to prevent the development of the cardiac disease phenotype.[19] Efficient *trans*-splicing depends on different factors, such as efficient delivery of PTMs to desired cell type and especially PTM design.[30] Increasing the number of viral particles used for transduction could be difficult, since at a certain point AAV turned to be toxic for the cells (data not shown). On the other hand, PTM design could be improved, particularly for the binding domain. To have approximately the same packaging size for the 5′ PTM and 3′ PTM, we chose to target intron 21 in the *MYBPC3* gene. The binding domain covered 120 nt (of 246) and was located roughly in the middle. However, we included highly conserved splice donor and acceptor sites in the 5′ PTM and 3′ PTM, respectively, which could be even stronger than the corresponding sequences in *MYBPC3* intron 21. We are aware that additional systematic testing of different lengths and complementary regions might have led to higher binding affinities for the endogenous pre-mRNA and, therefore, to higher *trans*-splicing efficiencies. Further optimization should be done in the future. Nevertheless, this is the first proof of concept of *trans*-splicing in hiPSC-CMs.

Gene replacement by cDNA overexpression is another very attractive treatment option for sarcomeric cardiomyopathies. Indeed, we recently demonstrated that AAV-mediated delivery of full-length WT *Mybpc3* cDNA in homozygous *Mybpc3*-targeted knockin mice not only prevented the development of cardiac hypertrophy and dysfunction, by increasing the amount of cMyBP-C protein, but also suppressed the expression of the endogenous mutant alleles.[21] Exogenous expression of a sarcomeric protein is expected to replace in part or completely the endogenous counterpart, since the sarcomere is a tightly regulated system with a preserved stoichiometry of all structural components.[46] This is the case in this study for the control cell line since *MYBPC3* gene transfer resulted in a 2.4-fold higher level of *MYBPC3* mRNA without change in the level of full-length cMyBP-C protein. Similarly, *MYBPC3* gene transfer resulted in a 2.6-fold higher amount of *MYBPC3* mRNA in HCM cells. Importantly and because the basal level was lower than in control cell lines, the cMyBP-C amount after gene transfer in HCM CMs reached 81% of the control cell line. In this condition, we expected at least a partial correction of the disease phenotype, since we previously showed that restoration of 80% of the cMyBP-C level by *MYBPC3* gene transfer partially restores the disease phenotype of engineered heart tissue derived from *Mybpc3*-deficient mice.[47] Indeed, the partial restoration

of cMyBP-C haploinsufficiency was sufficient to suppress hypertrophy in HCM CMs. Exogenous FLAG-cMyBP-C proteins were properly incorporated into the sarcomere in both cell lines. *MYBPC3* gene replacement had a positive effect on mRNA levels of proteins associated with hypertrophy or calcium handling. For instance, serum response factor (*SRF*) and *S100A4*, which are known to be higher in cardiomyopathies,[48,49] were significantly reduced after 7 days of *MYBPC3* therapy. In addition, levels of mRNAs encoding proteins belonging to the PI3K-Akt Kyoto Encyclopedia of Genes and Genome (KEGG) pathway, such as *CTGF*, collagens (*COL1A1* and *COL3A1*), and fibronectin (*FN1*), were significantly reduced. The mechanism by which the latter are regulated by gene therapy is not certain, but it could be related to paracrine factors mediating the crosstalk between CMs and fibroblasts (as reviewed elsewhere[50,51]). Finally, gene therapy increased mRNA levels of calcium-handling proteins, suggesting improvement of the cardiac contraction. We are aware that a weakness of the findings reported here concerns the comparison of the diseased line to an unrelated control and not to a corrected isogenic hiPSC line. However, in line with our findings, adenoviral-mediated *MYBPC3* gene delivery for 7 days restored the amount of cMyBP-C protein toward WT level and prevented hypertrophy in CMs derived from hESCs.[41]

In conclusion, our findings support gene replacement by overexpression of *MYBPC3* cDNA as a promising therapeutic option, particularly for infants with bi-allelic truncating *MYBPC3* mutations.[15–17] This causal therapy could prolong and improve quality of life of these affected infants for whom no other therapy exists except heart transplantation. The evaluation of the efficacy of therapeutic options in a human cellular model, such as hiPSC-CMs, represents an intermediate step toward clinical application for these infants. Further studies with large animal models of severe forms of cardiomyopathy are still required to test AAV doses and delivery before going to first-in patient.

MATERIALS AND METHODS

Vector Design

The 5′ PTM was obtained by fusion PCR of *MYBPC3* exon 1–21 coding sequence (PCR1) and the binding domain in intron 21 (PCR2) with partially overlapping primers. The list of primers is given in Table S2. The amplicon of PCR1 was obtained with a forward primer (F5-1) containing the *NheI* restriction site, the FLAG sequence, and the first 16 coding nt of *MYBPC3* exon 1. The reverse primer (R5-1) for PCR1 contained the BamHI restriction site, the downstream intronic splicing enhancer (DISE) element sequence, followed by the 5′ canonical splice donor site and the last 15 nt of *MYBPC3* exon 21. The *MYBPC3* coding sequence was amplified from the pSPORT-CMV-*MYBPC3,* clone BC151211.1 (Thermo Scientific). The amplicon of PCR2 was obtained with a forward primer (F5-2) containing a few nucleotides of the DISE, a BamHI restriction site, and 18 nt of intron 21. The reverse primer (R5-2) comprised an *NotI* restriction site and 18 nt of intron 21. Amplicons obtained in PCR1 and PCR2 were then used as templates for a third (fusion) PCR with primers F5-1 and R5-2. The 3′ PTM was obtained by fusion PCR of three different PCRs. PCR1 was performed to amplify the binding domain in intron 21 using a forward primer (F3-1) containing an *NheI* restriction site followed by 18 nt of *MYBPC3* intron 21 and a reverse primer (R3-1) comprising 14 nt of the linker sequence, a BamHI restriction site, and 18 nt of *MYBPC3* intron 21. PCR2 was performed to amplify the 3′ splicing sequences with forward primer F3-2 (same sequence as R3-1) and reverse primer (R3-2) carrying 10 nt of *MYBPC3* exon 22, 3′ canonical splice acceptor site sequence, and the polypyrimidine tract. PCR3 was performed to amplify the *MYBPC3* coding sequence from exon 22 to exon 34 with a forward primer F3-3 (same sequence as R3-2) and a reverse primer R3-3 carrying an *NotI* restriction site, the stop codon TGA, the FLAG sequence, and 12 nt of exon 34. PCR1 and PCR2 were then used as templates in PCR4 with primers F3-1 and R3-2 and finally PCR4 and PCR3 were fused in PCR5 with primers F3-1 and R3-3.

Production and Titration of AAV Particles

For production of AAV vectors, HEK293T cells were triple transfected with modified *rep2/cap9*-plasmid p5E18-VD-2/9-SLRSPPS,[34] plasmid pDGΔVP containing adenovirus helper functions, and one of the ITR-containing plasmids (scAAV-*TNNT2*-EGFP,[52] pGG2-*TNNT2*-FLAG-*MYBPC3*, pGG2-*TNNT2*-5′ PTM, or pGG2-*TNNT2*-3′ PTM, with FLAG-*MYBPC3*, 5′ PTM, and 3′ PTM inserted by *Nhe*I and *Not*I). Transfection, harvesting, and purification were performed as described previously.[34] In brief, cells were transfected with PEI (Polysciences), harvested after 48–72 hr cells by Trypsin-EDTA, and lysed in cell lysis buffer (50 mM Tris-Cl [pH 8.5], 150 mM NaCl, and 5 mM $MgCl_2$). Cell lysates were sonicated with a Sonorex TK device for 1 min at 48 W (Bandelin) and treated with 100 U Benzonase (Sigma-Aldrich) per milliliter of lysate for 30 min at 37°C. AAV particles were then purified by iodixanol density gradient ultracentrifugation, desalted (ZebaSpin desalting columns, recommended for processing compounds >7,000 Da [7 MWCO]; Thermo Fisher Scientific) from 40% iodixanol to 1× PBS, followed by concentration using Vivaspin6 columns (10 MWCO, Sartorius).

Generation of Patient-Specific hiPSC Line

The HCM patient was recruited in the outpatient clinic at the University Heart Center Hamburg and provided written informed consent for the use of fibroblasts. A skin biopsy was taken, washed in PBS, minced, and placed in a six-well plate in fibroblast medium (DMEM with 10% fetal bovine serum [FBS, PAA], 2 mM L-glutamine, and 0.5% penicillin and streptomycin; all Life Technologies). Dermal fibroblasts growing out of the explants were collected for passaging or cryopreservation and used for subsequent reprogramming at passage 5. The reprogramming was performed according to previously published protocols with retroviruses encoding the human transcription factors OCT3/4, SOX2, KLF4, and L-MYC.[53–55]

CM Differentiation, AAV Transduction, and Culture

CM differentiation from hiPSCs was performed following a three-step protocol with generation of embryoid bodies (EBs) in spinner flasks as described.[56,57] After dissociation with collagenase 2, beating CMs were transduced in suspension for 1 hr at 37°C with AAV at an MOI of 10,000. Transduced and non-transduced CMs were plated on

Geltrex-coated (1:100, Gibco) 12-well or 96-well plates at a density of 440,000 cells/well or 10,000 cells/well, respectively. CMs were maintained in culture as a monolayer in DMEM (10% heat inactivated fetal calf serum [FCS, Gibco], 0.1% insulin [Sigma-Aldrich], and 0.5% penicillin/streptomycin [Gibco]) for 7 days at 37°C and 10% CO_2 prior to further analyses.

Immunofluorescence Staining of hiPSC-CMs

Human iPSC-CMs were cultured for 7 days in 96-well plates (μclear, Greiner), then rinsed once with pre-warmed 1× PBS and fixed with Histofix (Carl Roth) for 20 min at 4°C. After washing two times in cold 1× PBS, hiPSC-CMs were incubated with primary antibodies directed against the M-motif of cMyBP-C (1:200, custom made), FLAG (1:800, Sigma), and α-actinin (1:800, Sigma); diluted in permeabilization buffer (1× PBS [Gibco], milk powder 3% [w/v, Carl Roth], and Triton X-100 0.1% [Carl Roth]); and incubated overnight at 4°C under gentle agitation. After washing two times in cold 1× PBS, hiPSC-CMs were incubated with secondary antibodies anti-mouse Alexa Fluor 488 (1:800, Life Technologies) and anti-rabbit Alexa Fluor 546 (1:800, Life Technologies), diluted in permeabilization buffer, and incubated for 1–2 hr at room temperature under gentle agitation and protected from light. In a final step, Hoechst 33342 (1:2,500, Thermo Fisher Scientific) diluted in 1× PBS was added to the wells and incubated for an additional 20 min. After washing two times in 1× PBS, hiPSC-CMs were ready for subsequent analysis in the Opera High-Content Screening System (PerkinElmer) or by confocal microscopy using a Zeiss LSM 800 microscope with Airyscan technology.

Measurement of CM Size

For quantification of hiPSC-CMs and for cell size analysis, the Opera High-Content Screening System and the Zeiss LSM 800 with Airyscan technology system were used. For Opera analysis, stained hiPSC-CMs in 96-well plates were loaded into the microscope, and, depending on how many wells were included in the analysis, 500–2,500 images were taken in 10× magnification. Those images were transferred in the Columbus Image Data Management and Analysis System (PerkinElmer). Columbus delivers pre-tested scripts, which were modified according to the characteristics of the used hiPSC-CMs. In this process, single building blocks were defined and accustomed to the hiPSC-CMs. Using the customized script, bulk analyses of the experiments were done and cell parameters of interest were obtained. For confocal microscopy, hiPSC-CMs were stained in 96-well plates and >100 images per sample were recorded, prepared according to the Opera analysis. Cell sizes from confocal images were measured by using Fiji software (ImageJ). Quality criteria for hiPSC-CM inclusion were set for single cells with well-formed sarcomeres.

RNA Isolation and Expression Analysis

Total RNA was extracted from hiPSC-CMs using TRIzol Reagent (Life Technologies), following the manufacturer's protocol. The conversion of cDNA was performed with SuperScript III First-Strand Synthesis System (Invitrogen), according to the manufacturer's instructions. For reverse transcription, oligo(dT) primers supplied in the kit and 200 ng extracted RNA were used. Touchdown RT-PCR to detect different *MYBPC3* transcripts in 5′ or 3′ *trans*-splicing experiments (63°C–58°C and 67°C–62°C, respectively) was performed using Phusion Hot Start II High-Fidelity DNA Polymerase (Thermo Fisher Scientific) in a total volume of 20 μL for 35 cycles, according to the instructions of the manufacturer's protocol. The qRT-PCR was performed in triplicates with SYBR-Green (Fermentas) according to the manufacturer's instructions. Glyceraldehyde 3-phosphate dehydrogenase (*GAPDH*) was used as the housekeeping gene. The target sequences were amplified during 40 cycles in an AbiPrism7000HT cycler (Applied Biosystems). For expression analysis with the nanoString nCounter Elements technology, a total amount of 50 ng RNA was hybridized with a customized nanoString Gene Expression CodeSet (Table S1) and analyzed using the nCounter Sprint Profiler. The mRNA levels were normalized to five housekeeping genes (*ABCF1*, *CLTC*, *GAPDH*, *PGK1*, and *TUBB*) and expressed as fold change in HCM over control CMs.

Western Blot

Western blot analysis was performed on total crude protein lysates from cultured hiPSC-CMs in the different conditions. Same amount of proteins (20 μg/lane) of single samples or pooled samples (n = 5–6) were separated on a 10% SDS-polyacrylamide (29:1) mini-gels (Bio-Rad) and transferred by wet-electroblotting to nitrocellulose membranes. Membranes were stained with the primary antibodies directed against the M-motif of cMyBP-C (polyclonal, 1:10,000, custom made) and α-actinin (monoclonal, 1:10,000, Sigma). Peroxidase-conjugated secondary antibodies against mouse (1:20,000, Dianova) or against rabbit (1:20,000, Sigma) were used. Proteins were visualized using Amersham ECL Prime Western Blotting Detection Reagent (GE Healthcare), and the signals were detected on Amersham Hyperfilm MP (GE Healthcare). Signals were quantified with GeneTools image analyzing software (Syngene).

Statistical Analysis

Data are presented as mean ± SEM. Statistical analyses were performed by Student's t test and two-way ANOVA with Bonferroni post-test using the GraphPad Prism 6.0 software. A value of $p < 0.05$ was considered significant.

SUPPLEMENTAL INFORMATION

Supplemental Information includes six figures and two tables and can be found with this article online at http://dx.doi.org/10.1016/j.omtn.2017.05.008.

AUTHOR CONTRIBUTIONS

Conceptualization, M. Prondzynski, G.M., and L.C.; Methodology, M. Prondzynski, G.M., and L.C.; Investigation, M. Prondzynski, E.K., and G.M.; Formal Analysis, M. Prondzynski, G.M., and L.C.; Visualization, M. Prondzynski; Resources, S.D.L., A.S., A.H., F.F., O.P., O.J.M., J.M., C.R., M. Patten, T.E., and L.C.; Writing – Original Draft, M. Prondzynski and G.M.; Writing – Review & Editing, M. Prondzynski, T.E., G.M., and L.C.; Project Administration,

M. Prondzynski, G.M., and L.C.; Supervision, G.M. and L.C.; Funding Acquisition, T.E., G.M., and L.C.

CONFLICTS OF INTEREST

L.C., T.E., O.J.M., and G.M. are co-authors of a provisional European patent application EP13164212, filed April 17, 2013, Gene-therapy vectors for treating cardiomyopathy, followed by an international patent US20160108430, application US 14/785,188, publication date April 21, 2016 (filing date April 17, 2014). The remaining authors declare no conflicts of interest.

ACKNOWLEDGMENTS

We are thankful to Alessandra Moretti (Department of Cardiology, Klinikum rechts der Isar, Technische Universität München) for providing the control hiPSC cell line. We would like to thank the cardiac differentiation team, especially Ingra Mannhardt-Vollert, Tessa Werner, and Bärbel Ulmer for precious help (UKE-Pharmacology) and Andreas Jungmann for support with AAV productions (Internal Medicine III, University Hospital Heidelberg). We also want to thank Oliver Keminer for his help and technical assistance with the Opera High-Content Screening System and the Columbus Image Data Management and Analysis System (Fraunhofer IME Screening-Port). Finally, we would like to thank Suellen Lopes Oliveira for graphic design (http://www.suelopes.com) and visualization. This work was supported by the DZHK (German Centre for Cardiovascular Research, the German Ministry of Research Education (BMBF), and by the Seventh Framework Program of the European Union (Health-F2-2009–241577; Big-Heart project).

REFERENCES

1. Hammond, S.M., and Wood, M.J. (2011). Genetic therapies for RNA mis-splicing diseases. Trends Genet. *27*, 196–205.
2. Doudna, J.A., and Charpentier, E. (2014). Genome editing. The new frontier of genome engineering with CRISPR-Cas9. Science *346*, 1258096.
3. Wang, D., and Gao, G. (2014). State-of-the-art human gene therapy: part I. Gene delivery technologies. Discov. Med. *18*, 67–77.
4. Semsarian, C., Ingles, J., Maron, M.S., and Maron, B.J. (2015). New perspectives on the prevalence of hypertrophic cardiomyopathy. J. Am. Coll. Cardiol. *65*, 1249–1254.
5. Elliott, P.M., Anastasakis, A., Borger, M.A., Borggrefe, M., Cecchi, F., Charron, P., Hagege, A.A., Lafont, A., Limongelli, G., Mahrholdt, H., et al.; Authors/Task Force members (2014). 2014 ESC Guidelines on diagnosis and management of hypertrophic cardiomyopathy: the Task Force for the Diagnosis and Management of Hypertrophic Cardiomyopathy of the European Society of Cardiology (ESC). Eur. Heart J. *35*, 2733–2779.
6. Behrens-Gawlik, V., Mearini, G., Gedicke-Hornung, C., Richard, P., and Carrier, L. (2014). MYBPC3 in hypertrophic cardiomyopathy: from mutation identification to RNA-based correction. Pflugers Arch. *466*, 215–223.
7. Carrier, L., Mearini, G., Stathopoulou, K., and Cuello, F. (2015). Cardiac myosin-binding protein C (MYBPC3) in cardiac pathophysiology. Gene *573*, 188–197.
8. Marston, S., Copeland, O., Jacques, A., Livesey, K., Tsang, V., McKenna, W.J., Jalilzadeh, S., Carballo, S., Redwood, C., and Watkins, H. (2009). Evidence from human myectomy samples that MYBPC3 mutations cause hypertrophic cardiomyopathy through haploinsufficiency. Circ. Res. *105*, 219–222.
9. Craig, R., Lee, K.H., Mun, J.Y., Torre, I., and Luther, P.K. (2014). Structure, sarcomeric organization, and thin filament binding of cardiac myosin-binding protein-C. Pflugers Arch. *466*, 425–431.
10. Sequeira, V., Witjas-Paalberends, E.R., Kuster, D.W., and van der Velden, J. (2014). Cardiac myosin-binding protein C: hypertrophic cardiomyopathy mutations and structure-function relationships. Pflugers Arch. *466*, 201–206.
11. Moss, R.L., Fitzsimons, D.P., and Ralphe, J.C. (2015). Cardiac MyBP-C regulates the rate and force of contraction in mammalian myocardium. Circ. Res. *116*, 183–192.
12. Marziliano, N., Merlini, P.A., Vignati, G., Orsini, F., Motta, V., Bandiera, L., Intrieri, M., and Veronese, S. (2012). A case of compound mutations in the MYBPC3 gene associated with biventricular hypertrophy and neonatal death. Neonatology *102*, 254–258.
13. Ho, C.Y., Lever, H.M., DeSanctis, R., Farver, C.F., Seidman, J.G., and Seidman, C.E. (2000). Homozygous mutation in cardiac troponin T: implications for hypertrophic cardiomyopathy. Circulation *102*, 1950–1955.
14. Maron, B.J., Maron, M.S., and Semsarian, C. (2012). Double or compound sarcomere mutations in hypertrophic cardiomyopathy: a potential link to sudden death in the absence of conventional risk factors. Heart Rhythm *9*, 57–63.
15. Wessels, M.W., Herkert, J.C., Frohn-Mulder, I.M., Dalinghaus, M., van den Wijngaard, A., de Krijger, R.R., Michels, M., de Coo, I.F., Hoedemaekers, Y.M., and Dooijes, D. (2015). Compound heterozygous or homozygous truncating MYBPC3 mutations cause lethal cardiomyopathy with features of noncompaction and septal defects. Eur. J. Hum. Genet. *23*, 922–928.
16. Lekanne Deprez, R.H., Muurling-Vlietman, J.J., Hruda, J., Baars, M.J., Wijnaendts, L.C., Stolte-Dijkstra, I., Alders, M., and van Hagen, J.M. (2006). Two cases of severe neonatal hypertrophic cardiomyopathy caused by compound heterozygous mutations in the MYBPC3 gene. J. Med. Genet. *43*, 829–832.
17. Xin, B., Puffenberger, E., Tumbush, J., Bockoven, J.R., and Wang, H. (2007). Homozygosity for a novel splice site mutation in the cardiac myosin-binding protein C gene causes severe neonatal hypertrophic cardiomyopathy. Am. J. Med. Genet. A. *143A*, 2662–2667.
18. Gedicke-Hornung, C., Behrens-Gawlik, V., Reischmann, S., Geertz, B., Stimpel, D., Weinberger, F., Schlossarek, S., Précigout, G., Braren, I., Eschenhagen, T., et al. (2013). Rescue of cardiomyopathy through U7snRNA-mediated exon skipping in Mybpc3-targeted knock-in mice. EMBO Mol. Med. *5*, 1128–1145.
19. Mearini, G., Stimpel, D., Krämer, E., Geertz, B., Braren, I., Gedicke-Hornung, C., Précigout, G., Müller, O.J., Katus, H.A., Eschenhagen, T., et al. (2013). Repair of Mybpc3 mRNA by 5′-trans-splicing in a Mouse Model of Hypertrophic Cardiomyopathy. Mol. Ther. Nucleic Acids *2*, e102.
20. Jiang, J., Wakimoto, H., Seidman, J.G., and Seidman, C.E. (2013). Allele-specific silencing of mutant Myh6 transcripts in mice suppresses hypertrophic cardiomyopathy. Science *342*, 111–114.
21. Mearini, G., Stimpel, D., Geertz, B., Weinberger, F., Krämer, E., Schlossarek, S., Mourot-Filiatre, J., Stoehr, A., Dutsch, A., Wijnker, P.J., et al. (2014). *Mybpc3* gene therapy for neonatal cardiomyopathy enables long-term disease prevention in mice. Nat. Commun. *5*, 5515.
22. Moretti, A., Bellin, M., Welling, A., Jung, C.B., Lam, J.T., Bott-Flügel, L., Dorn, T., Goedel, A., Höhnke, C., Hofmann, F., et al. (2010). Patient-specific induced pluripotent stem-cell models for long-QT syndrome. N. Engl. J. Med. *363*, 1397–1409.
23. Lahti, A.L., Kujala, V.J., Chapman, H., Koivisto, A.P., Pekkanen-Mattila, M., Kerkelä, E., Hyttinen, J., Kontula, K., Swan, H., Conklin, B.R., et al. (2012). Model for long QT syndrome type 2 using human iPS cells demonstrates arrhythmogenic characteristics in cell culture. Dis. Model. Mech. *5*, 220–230.
24. Hinson, J.T., Chopra, A., Nafissi, N., Polacheck, W.J., Benson, C.C., Swist, S., Gorham, J., Yang, L., Schafer, S., Sheng, C.C., et al. (2015). HEART DISEASE. Titin mutations in iPS cells define sarcomere insufficiency as a cause of dilated cardiomyopathy. Science *349*, 982–986.
25. Sun, N., Yazawa, M., Liu, J., Han, L., Sanchez-Freire, V., Abilez, O.J., Navarrete, E.G., Hu, S., Wang, L., Lee, A., et al. (2012). Patient-specific induced pluripotent stem cells as a model for familial dilated cardiomyopathy. Sci. Transl. Med. *4*, 130ra47.
26. Gramlich, M., Pane, L.S., Zhou, Q., Chen, Z., Murgia, M., Schötterl, S., Goedel, A., Metzger, K., Brade, T., Parrotta, E., et al. (2015). Antisense-mediated exon skipping: a therapeutic strategy for titin-based dilated cardiomyopathy. EMBO Mol. Med. *7*, 562–576.
27. Lan, F., Lee, A.S., Liang, P., Sanchez-Freire, V., Nguyen, P.K., Wang, L., Han, L., Yen, M., Wang, Y., Sun, N., et al. (2013). Abnormal calcium handling properties underlie

familial hypertrophic cardiomyopathy pathology in patient-specific induced pluripotent stem cells. Cell Stem Cell *12*, 101–113.

28. Ojala, M., Prajapati, C., Pölönen, R.P., Rajala, K., Pekkanen-Mattila, M., Rasku, J., Larsson, K., and Aalto-Setälä, K. (2016). Mutation-Specific Phenotypes in hiPSC-Derived Cardiomyocytes Carrying Either Myosin-Binding Protein C Or α-Tropomyosin Mutation for Hypertrophic Cardiomyopathy. Stem Cells Int. *2016*, 1684792.

29. Tanaka, A., Yuasa, S., Mearini, G., Egashira, T., Seki, T., Kodaira, M., Kusumoto, D., Kuroda, Y., Okata, S., Suzuki, T., et al. (2014). Endothelin-1 induces myofibrillar disarray and contractile vector variability in hypertrophic cardiomyopathy-induced pluripotent stem cell-derived cardiomyocytes. J. Am. Heart Assoc. *3*, e001263.

30. Berger, A., Maire, S., Gaillard, M.C., Sahel, J.A., Hantraye, P., and Bemelmans, A.P. (2016). mRNA trans-splicing in gene therapy for genetic diseases. Wiley Interdiscip. Rev. RNA *7*, 487–498.

31. Wally, V., Murauer, E.M., and Bauer, J.W. (2012). Spliceosome-mediated trans-splicing: the therapeutic cut and paste. J. Invest. Dermatol. *132*, 1959–1966.

32. Wang, D., and Gao, G. (2014). State-of-the-art human gene therapy: part II. Gene therapy strategies and clinical applications. Discov. Med. *18*, 151–161.

33. Collins, M., and Thrasher, A. (2015). Gene therapy: progress and predictions. Proc. Biol. Sci. *282*, 20143003.

34. Varadi, K., Michelfelder, S., Korff, T., Hecker, M., Trepel, M., Katus, H.A., Kleinschmidt, J.A., and Müller, O.J. (2012). Novel random peptide libraries displayed on AAV serotype 9 for selection of endothelial cell-directed gene transfer vectors. Gene Ther. *19*, 800–809.

35. Lorain, S., Peccate, C., Le Hir, M., and Garcia, L. (2010). Exon exchange approach to repair Duchenne dystrophin transcripts. PLoS ONE *5*, e10894.

36. Ma, D., Wei, H., Lu, J., Ho, S., Zhang, G., Sun, X., Oh, Y., Tan, S.H., Ng, M.L., Shim, W., et al. (2013). Generation of patient-specific induced pluripotent stem cell-derived cardiomyocytes as a cellular model of arrhythmogenic right ventricular cardiomyopathy. Eur. Heart J. *34*, 1122–1133.

37. Dambrot, C., Braam, S.R., Tertoolen, L.G., Birket, M., Atsma, D.E., and Mummery, C.L. (2014). Serum supplemented culture medium masks hypertrophic phenotypes in human pluripotent stem cell derived cardiomyocytes. J. Cell. Mol. Med. *18*, 1509–1518.

38. Wang, G., McCain, M.L., Yang, L., He, A., Pasqualini, F.S., Agarwal, A., Yuan, H., Jiang, D., Zhang, D., Zangi, L., et al. (2014). Modeling the mitochondrial cardiomyopathy of Barth syndrome with induced pluripotent stem cell and heart-on-chip technologies. Nat. Med. *20*, 616–623.

39. Karakikes, I., Stillitano, F., Nonnenmacher, M., Tzimas, C., Sanoudou, D., Termglinchan, V., Kong, C.W., Rushing, S., Hansen, J., Ceholski, D., et al. (2015). Correction of human phospholamban R14del mutation associated with cardiomyopathy using targeted nucleases and combination therapy. Nat. Commun. *6*, 6955.

40. Walsh, R., Thomson, K.L., Ware, J.S., Funke, B.H., Woodley, J., McGuire, K.J., Mazzarotto, F., Blair, E., Seller, A., Taylor, J.C., et al. (2017). Reassessment of Mendelian gene pathogenicity using 7,855 cardiomyopathy cases and 60,706 reference samples. Genet. Med. *19*, 192–203.

41. Monteiro da Rocha, A., Guerrero-Serna, G., Helms, A., Luzod, C., Mironov, S., Russell, M., Jalife, J., Day, S.M., Smith, G.D., and Herron, T.J. (2016). Deficient cMyBP-C protein expression during cardiomyocyte differentiation underlies human hypertrophic cardiomyopathy cellular phenotypes in disease specific human ES cell derived cardiomyocytes. J. Mol. Cell. Cardiol. *99*, 197–206.

42. Marston, S., Copeland, O., Gehmlich, K., Schlossarek, S., and Carrier, L. (2012). How do MYBPC3 mutations cause hypertrophic cardiomyopathy? J. Muscle Res. Cell Motil. *33*, 75–80.

43. Vignier, N., Schlossarek, S., Fraysse, B., Mearini, G., Krämer, E., Pointu, H., Mougenot, N., Guiard, J., Reimer, R., Hohenberg, H., et al. (2009). Nonsense-mediated mRNA decay and ubiquitin-proteasome system regulate cardiac myosin-binding protein C mutant levels in cardiomyopathic mice. Circ. Res. *105*, 239–248.

44. Nagy, E., and Maquat, L.E. (1998). A rule for termination-codon position within intron-containing genes: when nonsense affects RNA abundance. Trends Biochem. Sci. *23*, 198–199.

45. van Dijk, S.J., Dooijes, D., dos Remedios, C., Michels, M., Lamers, J.M., Winegrad, S., Schlossarek, S., Carrier, L., ten Cate, F.J., Stienen, G.J., and van der Velden, J. (2009). Cardiac myosin-binding protein C mutations and hypertrophic cardiomyopathy: haploinsufficiency, deranged phosphorylation, and cardiomyocyte dysfunction. Circulation *119*, 1473–1483.

46. Tardiff, J.C., Carrier, L., Bers, D.M., Poggesi, C., Ferrantini, C., Coppini, R., Maier, L.S., Ashrafian, H., Huke, S., and van der Velden, J. (2015). Targets for therapy in sarcomeric cardiomyopathies. Cardiovasc. Res. *105*, 457–470.

47. Wijnker, P.J., Friedrich, F.W., Dutsch, A., Reischmann, S., Eder, A., Mannhardt, I., Mearini, G., Eschenhagen, T., van der Velden, J., and Carrier, L. (2016). Comparison of the effects of a truncating and a missense MYBPC3 mutation on contractile parameters of engineered heart tissue. J. Mol. Cell. Cardiol. *97*, 82–92.

48. Doroudgar, S., Quijada, P., Konstandin, M., Ilves, K., Broughton, K., Khalafalla, F.G., Casillas, A., Nguyen, K., Gude, N., Toko, H., et al. (2016). S100A4 protects the myocardium against ischemic stress. J. Mol. Cell. Cardiol. *100*, 54–63.

49. Zhang, X., Azhar, G., Chai, J., Sheridan, P., Nagano, K., Brown, T., Yang, J., Khrapko, K., Borras, A.M., Lawitts, J., et al. (2001). Cardiomyopathy in transgenic mice with cardiac-specific overexpression of serum response factor. Am. J. Physiol. Heart Circ. Physiol. *280*, H1782–H1792.

50. Mooren, F.C., Viereck, J., Krüger, K., and Thum, T. (2014). Circulating microRNAs as potential biomarkers of aerobic exercise capacity. Am. J. Physiol. Heart Circ. Physiol. *306*, H557–H563.

51. Takeda, N., and Manabe, I. (2011). Cellular Interplay between Cardiomyocytes and Nonmyocytes in Cardiac Remodeling. Int. J. Inflamm. *2011*, 535241.

52. Werfel, S., Jungmann, A., Lehmann, L., Ksienzyk, J., Bekeredjian, R., Kaya, Z., Leuchs, B., Nordheim, A., Backs, J., Engelhardt, S., et al. (2014). Rapid and highly efficient inducible cardiac gene knockout in adult mice using AAV-mediated expression of Cre recombinase. Cardiovasc. Res. *104*, 15–23.

53. Takahashi, K., Okita, K., Nakagawa, M., and Yamanaka, S. (2007). Induction of pluripotent stem cells from fibroblast cultures. Nat. Protoc. *2*, 3081–3089.

54. Takahashi, K., Tanabe, K., Ohnuki, M., Narita, M., Ichisaka, T., Tomoda, K., and Yamanaka, S. (2007). Induction of pluripotent stem cells from adult human fibroblasts by defined factors. Cell *131*, 861–872.

55. Ohnuki, M., Takahashi, K., and Yamanaka, S. (2009). Generation and characterization of human induced pluripotent stem cells. Curr. Protoc. Stem Cell Biol. *Chapter 4*, Unit 4A.2.

56. Mannhardt, I., Breckwoldt, K., Letuffe-Brenière, D., Schaaf, S., Schulz, H., Neuber, C., Benzin, A., Werner, T., Eder, A., Schulze, T., et al. (2016). Human Engineered Heart Tissue: Analysis of Contractile Force. Stem Cell Reports *7*, 29–42.

57. Breckwoldt, K., Letuffe-Brenière, D., Mannhardt, I., Schulze, T., Ulmer, B., Werner, T., Benzin, A., Klampe, B., Reinsch, M.C., Laufer, S., et al. (2017). Differentiation of cardiomyocytes and generation of human engineered heart tissue. Nat. Protoc. *12*, 1177–1197.

OMTN, Volume *7*

Supplemental Information

Evaluation of *MYBPC3 trans*-Splicing and Gene Replacement as Therapeutic Options in Human iPSC-Derived Cardiomyocytes

Maksymilian Prondzynski, Elisabeth Krämer, Sandra D. Laufer, Aya Shibamiya, Ole Pless, Frederik Flenner, Oliver J. Müller, Julia Münch, Charles Redwood, Arne Hansen, Monica Patten, Thomas Eschenhagen, Giulia Mearini, and Lucie Carrier

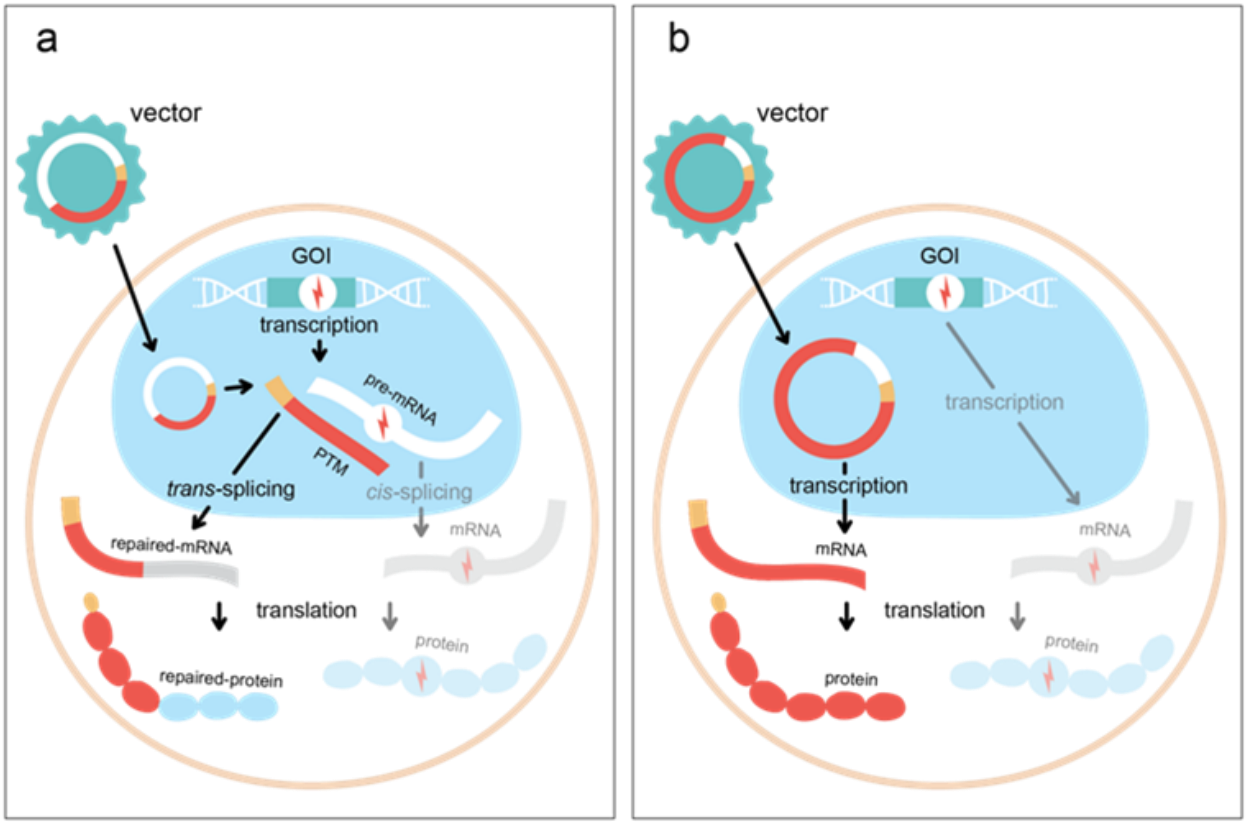

Figure S1: Schematic representation of two gene therapy approaches. (a) RNA *trans*-splicing. After virus-mediated delivery, pre-*trans*-splicing molecules (PTMs) are transcribed in the nucleus. PTMs target the pre-mRNA of the gene of interest (GOI) and produce via *trans*-splicing a repaired, chimeric mRNA, without mutation. Translation of the repaired mRNA leads to a corrected fully functional protein. This process is competing with *cis*-splicing, the classical splicing mechanism, by which endogenous mRNA and proteins are produced. **(b)** Gene replacement. The mutation in the GOI results in low level or the absence of corresponding protein. After virus-mediated delivery, a full-length wild-type cDNA of GOI is transcribed in the nucleus. The resulting mRNA is translated into functional protein that replaces the missing mutant endogenous protein. GOI: gene of interest; yellow tag: i.e. FLAG to discriminate exogenous molecules; red bolt: gene mutation.

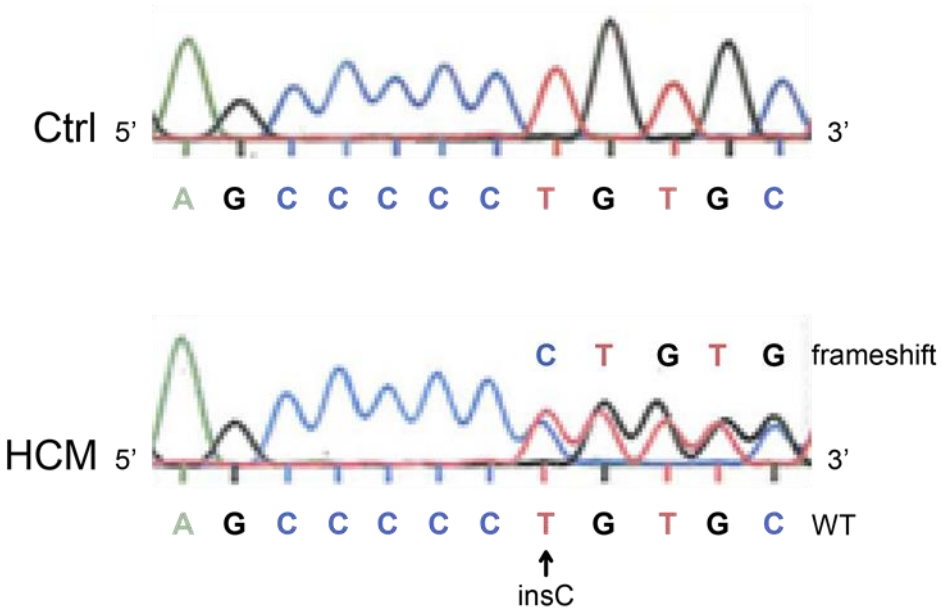

Figure S2: Validation of the *MYBPC3* mutation at the genomic level. PCR was performed on genomic DNA from blood cells from the HCM patient using intronic primers around *MYBPC3* exon 16 and compared to a human control sequence. Sanger sequencing confirmed the presence of an insertion of a C (c.1358_1359insC) at the heterozygous state in the HCM patient. Wild-type and frameshift sequences are also shown.

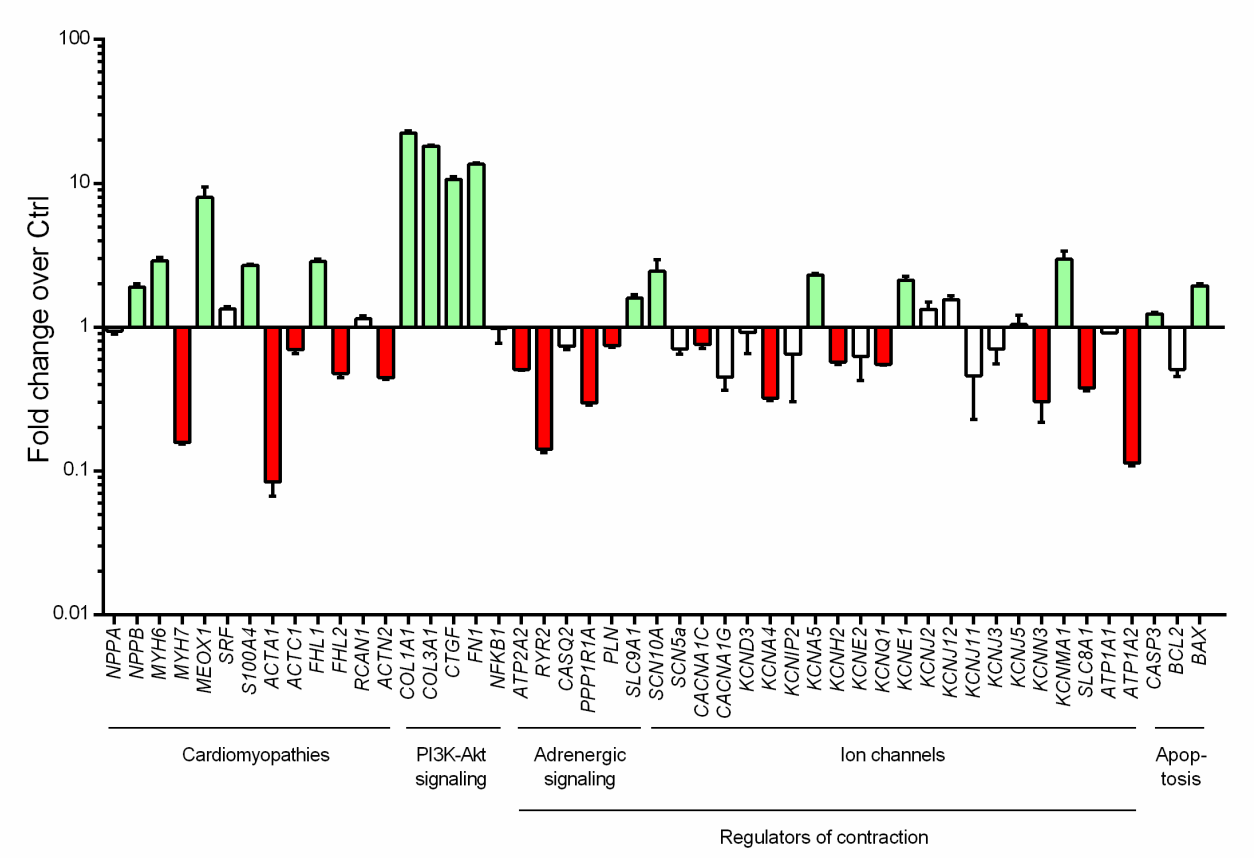

Figure S3: Gene expression analysis of Ctrl and HCM hiPSC-derived cardiomyocytes. Evaluation of mRNA levels determined by nCounter NanoString technology in Ctrl and HCM hiPSC-derived CM (n=3-6, with n=number of wells from one transduction experiment). Green bars are significantly upregulated and red bars are significantly downregulated. Data are expressed as mean ± SEM. $P<0.05$, unpaired Students *t*-test.

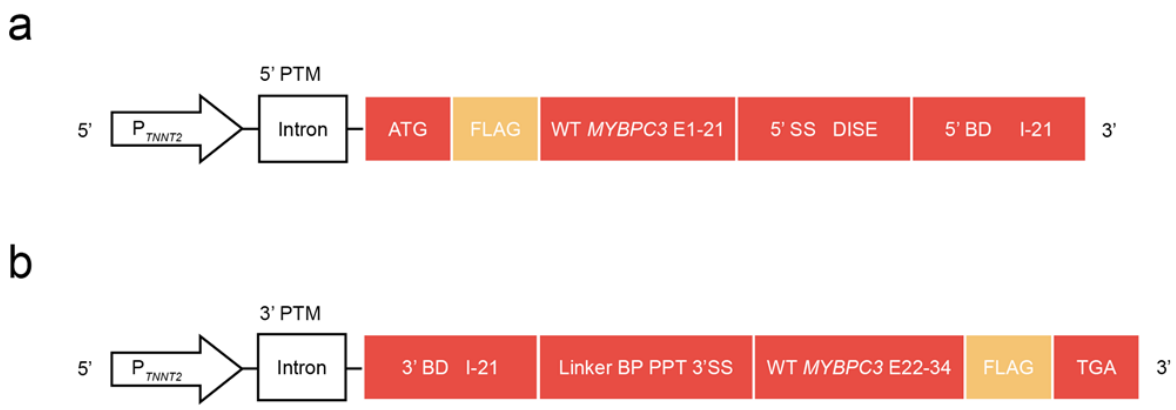

Figure S4: Schematic illustration of PTMs. (a) The 5'PTM plasmid carries the 5'-FLAG-tagged wild-type (WT) *MYBPC3* coding sequence of exons 1 to 21 under the control of the human cardiac troponin T promoter (*TNNT2*). The 5'PTM also included a chimeric intron, containing sequences from the human β-globin and immunoglobulin (IgG) genes, conserved splice donor site (5'SS) followed by an intronic region (DISE) from the rat fibroblast growth factor receptor 2 gene and 120 nucleotides for binding to *MYBPC3* intron 21 (5' BD I-21). **(b)** The 3'PTM plasmid carries wild-type (WT) *MYBPC3* coding sequence of exons 22 to 34 under the control of the human cardiac troponin T promoter (*TNNT2*). The sequence is FLAG-tagged at the 3' end before the stop codon (TGA). The 3'PTM includes the same intron as in (a) and the binding domain targets the same sequence in *MYBPC3* intron 21 as 5'PTM. In addition, conserved 3' splicing sequences such as branch point (BP) and polypyrimidine tract (PTT) are present. ATG, start codon; BP, branch point; DISE, downstream intronic splicing enhancer element; P_{TNNT2}, cardiac troponin T promoter; PPT, polypyrimidine tract; TGA, stop codon; 5´SS, 5´-splice site; 3´SS, 3´-splice site.

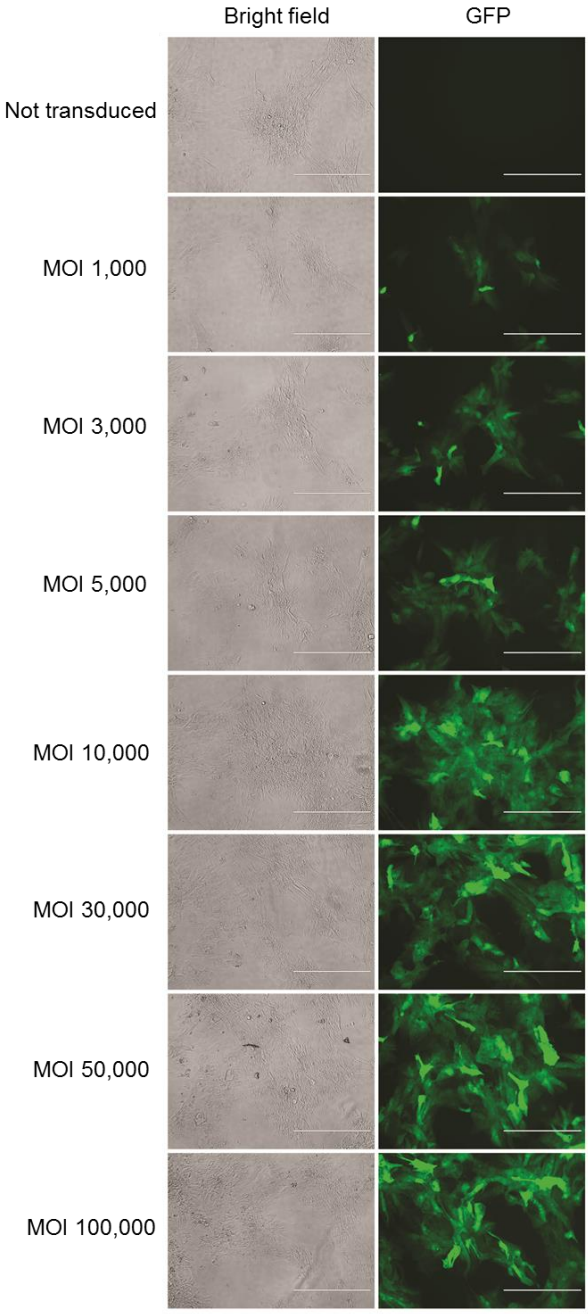

Figure S5: Efficiency of AAV-*TNNT2*-GFP-mediated transduction in control hiPSC-derived cardiomyocytes. hiPSC-CMs were transduced with MOIs of 1,000 up to 100,000 and cultured in 2D for seven days. GFP expression was evaluated by epifluorescence microscopy. Corresponding bright field images are also shown. Scale bars, 400 µm. GFP, green fluorescent protein; MOI, multiplicity of infection.

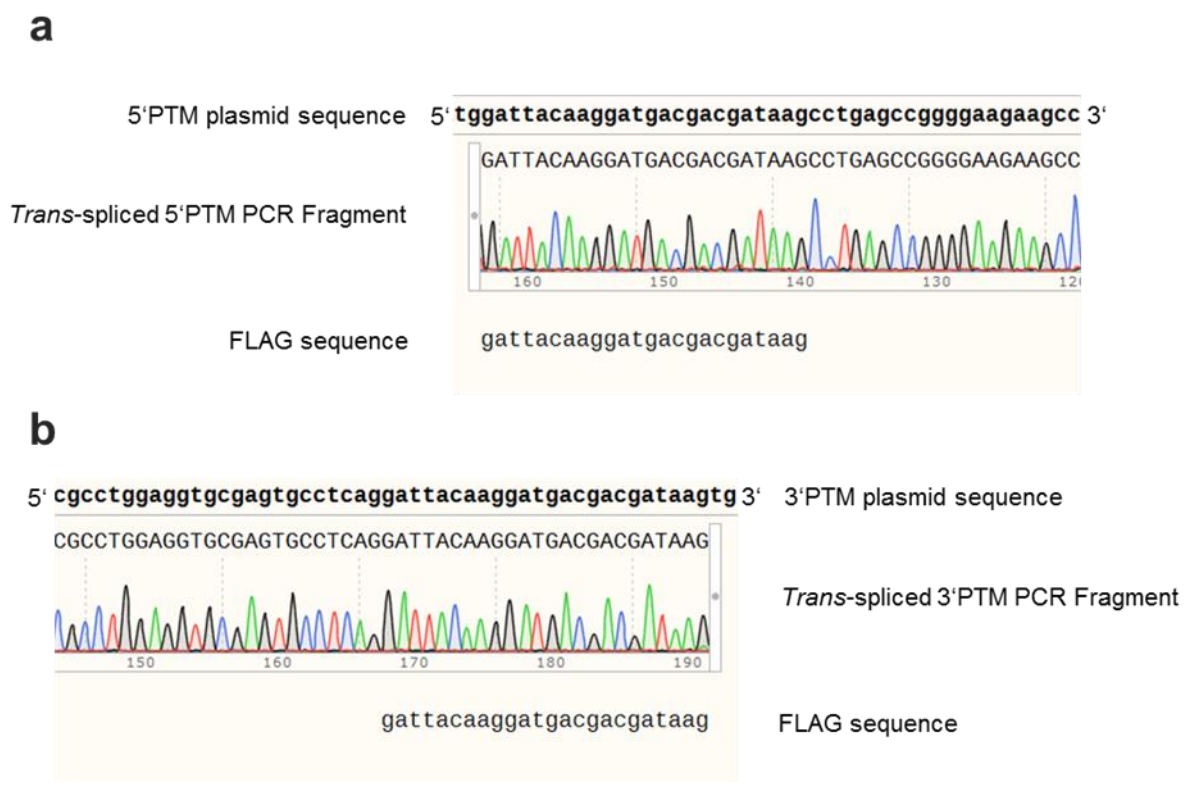

Figure S6: Validation of *trans*-spliced *MYBPC3* mRNA after 5’- and 3’-mode of *trans*-splicing. (a) Sequencing of the gel-extracted 2,180-bp fragment amplified by RT-PCR with primers FLAG-F/E23-R in the AAV-5’PTM-transduced hiPSC-CMs sample validated the presence of the FLAG sequence after alignment with the 5’PTM plasmid. **(b)** Sequencing of the gel-extracted 1,874-bp fragment amplified by RT-PCR with primers E21-F/FLAG-R in AAV-3’PTM-transduced hiPSC-CMs sample validated the presence of the FLAG sequence after alignment with the 3’PTM. Alignment was performed with SnapGene® software. E, exon; RT-PCR, reverse transcriptase PCR.

Supplemental Table S1. Acronyms and names of genes evaluated with the nanoString nCounter® Elements technology.

Acronym	Name	Accession number (NCBI)
ABCF1	ATP binding cassette subfamily F member 1	NM_001090.2
ACTA1	Actin, alpha, skeletal muscle	NM_001100.3
ACTC1	Actin, alpha, cardiac muscle 1	NM_005159.4
ACTN2	Alpha-Actinin 2	NM_001103.2
ATP1A1	Na/K-ATPase α1 subunit	NM_000702.3
ATP1A2	Na/K-ATPase α2 subunit	NM_001681.3
ATP2A2	ATPase sarcoplasmic/endoplasmic reticulum Ca2+ transporting 2	NM_001681.3
BAX	BCL2 associated X, apoptosis regulator	NM_138761.3
BCL2	BCL2, apoptosis regulator	NM_000657.2
CACNA1C	Calcium voltage-gated channel subunit alpha1 C (L-Type Ca2+ channel)	NM_199460.2
CACNA1G	Calcium voltage-gated channel subunit alpha1 G (T type Ca2+ channel)	NM_198397.1
CASP3	Caspase 3	NM_032991.2
CASQ2	Calsequestrin-2	NM_001232.3
CLTC	Clathrin heavy chain	NM_004859.2
COL1A1	Collagen type I alpha 1	NM_000088.3
COL3A1	Collagen type III alpha 1	NM_000090.3
CTGF	Connective tissue growth factor	NM_001901.2
FHL1	Four-and-a-half-LIM-domains 1	NM_001449.4
FHL2	Four-and-a-half-LIM-domains 2	NM_001039492.2
FN1	Fibronectin 1	NM_212482.1
GAPDH	Glyceraldehyde-3-phosphate dehydrogenase	NM_002046.3
KCNA4	Potassium voltage-gated channel subfamily A member 4 (Ito,s K+ channel)	NM_002233.3
KCNA5	Potassium voltage-gated channel subfamily A member 5 (IKUR)	NM_002234.2
KCND3	Potassium voltage-gated channel subfamily D member 3 (Ito, f beta subunit, Kv4.3)	NM_004980.4
KCNE1	Potassium voltage-gated channel subfamily E regulatory subunit 1 (MinK, Iks)	NM_001127670.1
KCNE2	Potassium voltage-gated channel subfamily E regulatory subunit 2 (MIRP2, Ikr)	NM_172201.1
KCNH2	Potassium voltage-gated channel subfamily H member 2 (Ikr K+ channel)	NM_172057.2
KCNIP2	Potassium voltage-gated channel interacting protein 2 (KChiP2 beta subunit, Ito)	NM_014591.4
KCNJ11	Potassium voltage-gated channel subfamily J member 11 (Kir 6.2, IkATP)	NM_000525.3
KCNJ12	Potassium voltage-gated channel subfamily J member 12 (Ik1 channel subunit 2)	NM_021012.4
KCNJ2	Potassium voltage-gated channel subfamily J member 2 (Ik1 channel)	NM_000891.2
KCNJ3	Potassium voltage-gated channel subfamily J member 3 (IKACH)	NM_001260508.1
KCNJ5	Potassium voltage-gated channel subfamily J member 5 (IKACH)	NM_000890.3
KCNMA1	Potassium calcium-activated channel subfamily M alpha 1 (BK Channel)	NM_001014797.2
KCNN3	Potassium calcium-activated channel subfamily N member 3 (SK3)	NM_002249.4
KCNQ1	Potassium voltage-gated channel subfamily Q member 1 (Iks K+ channel)	NM_181798.1
MEOX1	Mesenchyme homeobox 1	NM_001040002.1
MYH6	Myosin heavy chain 6	NM_002471.3
MYH7	Myosin heavy chain 7	NM_000257.2
NFKB1	Nuclear factor kappa B subunit 1	NM_003998.2
NPPA	Natriuretic peptide A	NM_006172.2
NPPB	Natriuretic peptide B	NM_002521.2
PGK1	Phosphoglycerate kinase 1	NM_000291.2
PLN	Phospholamban	NM_002667.3
PPP1R1A	Protein phosphatase 1, regulatory (inhibitor) subunit 1A (I-1)	NM_006741.3
RCAN1	Regulator of calcineurin 1	NM_004414.5
RYR2	Ryanodine receptor 2	NM_001035.2
S100A4	S100 calcium binding protein A4 (=FSP1)	NM_002961.2
SCN10A	Sodium voltage-gated channel alpha subunit 10 (Na+ channel, Nav1.8)	NM_006514.2
SCN5A	Sodium voltage-gated channel alpha subunit 5 (Na+ channel, Nav1.5)	NM_198056.2
SLC8A1	Solute carrier family 8 member A1 (Natrium-Calcium Exchanger, NCX)	NM_021097.1
SLC9A1	Solute carrier family 9 member A1 (Na+/H+ exchanger)	NM_003047.4
SRF	Serum response factor	NM_003131.3
TUBB	Tubulin beta class 1	NM_178014.3

Supplemental Table S2. Sequences of PCR primers

Primer	Sequence (5' to 3')
E1-F	GCCAGTCTCAGCTTTTAGCAA
E2-R	CAGGCCGTACTTGTTGCTG
I15-F	CTGGGACCTGAGGATGTGGG
I16-R	GGTGGGTGGGTGGCAAGTG
E15-F	CCAAGCGTACCCTGACCA
E16-R	CCCTCCTCCGATACTTCACA
E21-F	CCATTGTGGTTGTAGCTGGA
E23-R	CACACAGCAGCTTCTTGTCA
E33-F	CCCAAGATTTCCTGGTTCAAA
E33-R	CCTCGCCCTGTAAGTTGGT
FLAG-F	GGATTACAAGGATGACGACGA
FLAG-R	CTTATCGTCGTCATCCTTGTAATC
GAPDH-F	ATGTTCGTCATGGGTGTGAA
GAPDH-R	TGAGTCCTTCCACGATACCA
F3-1	TTCGACGCTAGCACCCACACTGCCCACCTT
R3-1	TGTTCCGCGGGGATCCTGTGTGGAACCAGCCAAG
F3-2	GTTCCACACAGGATCCCCGCGGAACATTATTATAAC
R3-2	CCTTATTCCCCTGTTTTCCGGAAA
F3-3	TTCCGGAAAACAGGGGAATAAGGC
R3-3	TTCGACGCGGCCGCTCACTTATCGTCGTCATCCTTGTAATCCTGAGGCACTCG
F5-1	TTCGACGCTAGCATGGATTACAAGGATGACGACGATAAGCCTGAGCCGGGGAAGA
R5-1	AGTGTGGGTGGATCCAGGCCAACCCATGGAAAGAAAGAGCTGTACTCACCTGCGTGATAGCCTTCTG
F5-2	GGGTTGGCCTGGATCCACCCACACTGCCCACCTT
R5-2	TTCGACGCGGCCGCTGTGTGGAACCAGCCAAG